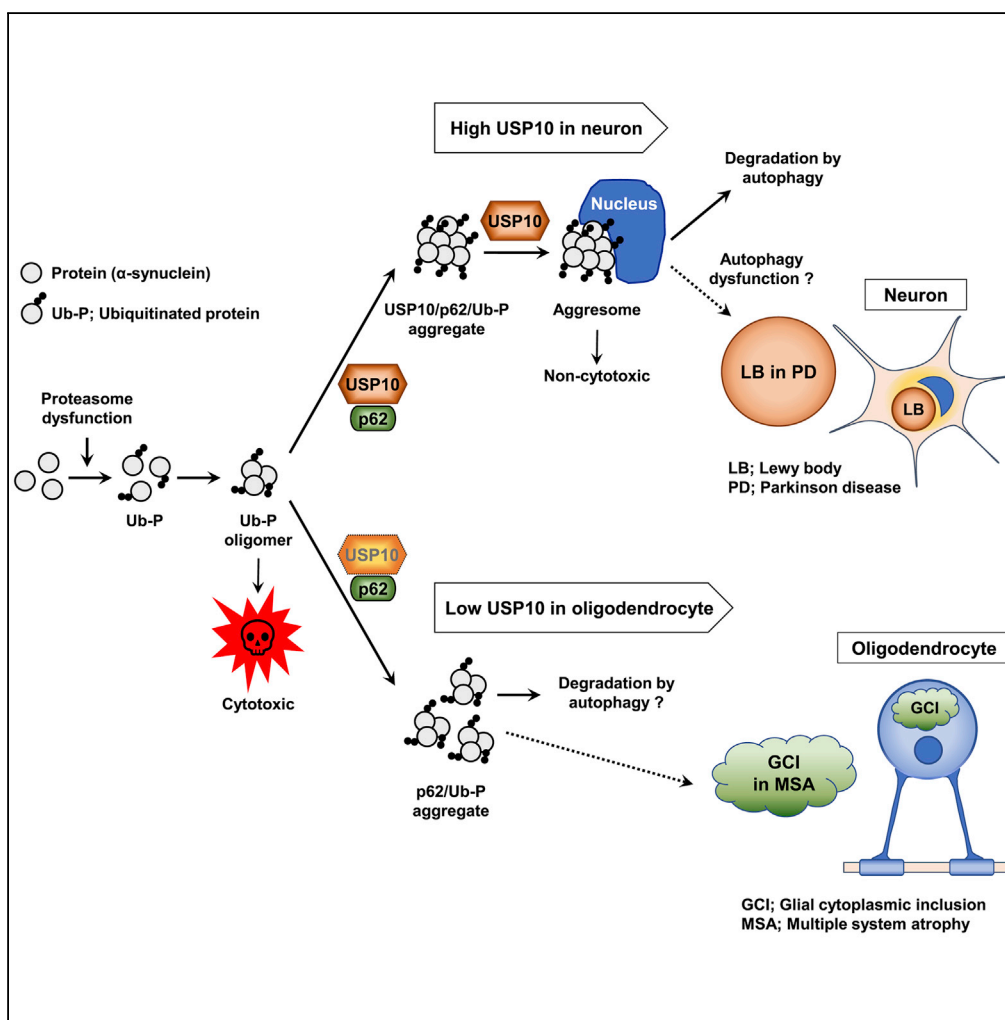


Article

USP10 Is a Driver of Ubiquitinated Protein Aggregation and Aggresome Formation to Inhibit Apoptosis



Masahiko Takahashi, Hiroki Kitaura, Akiyoshi Kakita, ..., Masaya Higuchi, Masaaki Komatsu, Masahiro Fujii

fujimas@med.niigata-u.ac.jp

HIGHLIGHTS

USP10 induces ubiquitinated protein aggregation and aggresome formation

USP10 inhibits ubiquitinated protein-induced apoptosis by aggresome formation

USP10 induces α-synuclein-positive aggresome

USP10 is colocalized with α-synuclein in Lewy body in Parkinson disease

Takahashi et al., iScience 9, 433–450
November 30, 2018 © 2018 The Authors.
<https://doi.org/10.1016/j.isci.2018.11.006>



Article

USP10 Is a Driver of Ubiquitinated Protein Aggregation and Aggresome Formation to Inhibit Apoptosis

Masahiko Takahashi,¹ Hiroki Kitaura,² Akiyoshi Kakita,² Taichi Kakihana,¹ Yoshinori Katsuragi,¹ Masaaki Nameta,³ Lu Zhang,² Yuriko Iwakura,⁴ Hiroyuki Nawa,⁴ Masaya Higuchi,⁵ Masaaki Komatsu,⁶ and Masahiro Fujii^{1,7,*}

SUMMARY

Accumulation of ubiquitinated proteins is cytotoxic, but cells inactivate these cytotoxicities by inducing aggresome formation. We found that ubiquitin-specific protease 10 (USP10) inhibits ubiquitinated protein-induced apoptosis by inducing aggresome formation. USP10 interacted with the ubiquitin receptor p62 and the interaction augmented p62-dependent ubiquitinated protein aggregation and aggresome formation, thereby cooperatively inhibiting apoptosis. We provide evidence that USP10/p62-induced protein aggregates inhibit proteasome activity, which increases the amount of ubiquitinated proteins and promotes aggresome formation. USP10 induced aggresomes containing α -synuclein, a pathogenic protein in Parkinson disease, in cultured cells. In Parkinson disease brains, USP10 was colocalized with α -synuclein in the disease-linked aggresome-like inclusion Lewy bodies, suggesting that USP10 inhibits α -synuclein-induced neurotoxicity by promoting Lewy body formation. Collectively, these findings suggest that USP10 is a critical factor to control protein aggregation, aggresome formation, and cytotoxicity in protein-aggregation-related diseases.

INTRODUCTION

Various stresses such as oxidative stress generate ubiquitinated proteins with high cytotoxicity. In addition, age-related impairment of proteasome activity causes accumulation of ubiquitinated proteins, which is also associated with cell death. Aberrant accumulation of ubiquitinated proteins as inclusions is a hallmark pathology of several age-related degenerative diseases such as Parkinson disease (PD) and cystic fibrosis (Luciani et al., 2010; Ross and Poirier, 2004). Thus, cells should inactivate the cytotoxicities of ubiquitinated proteins and simultaneously reduce their amount. However, how cells inactivate the cytotoxicities of these ubiquitinated proteins and how pathogenic inclusions are formed in age-related degenerative diseases is poorly understood.

Cells activate two intracellular defense systems to inactivate the cytotoxicities of ubiquitinated proteins: the aggresome-autophagy system and the ubiquitin-proteasome system. Aggresomes are stress-inducible aggregates consisting of ubiquitinated proteins, chaperones, and proteasome components, which share many characters with pathogenic inclusions in age-related degenerative diseases (Garcia-Mata et al., 1999; Kopito, 2000; Olanow et al., 2004). p62, histone deacetylase 6 (HDAC6) and dynein play critical roles in aggresome formation. p62 is a ubiquitin receptor that interacts with ubiquitinated proteins (Katsuragi et al., 2015). Such p62-bound ubiquitinated protein aggregates interact with microtubule-associated deacetylase HDAC6, and this complex is transported to the cytoplasmic perinuclear region (microtubule-organizing center) to form aggresomes by the functions of HDAC6 and dynein motor protein in a microtubule-dependent manner (Kawaguchi et al., 2003). Aggresomes are tightly linked to selective autophagy (aggrephagy), and multiple components recruited in aggresomes are degraded by p62-dependent selective autophagy (Johansen and Lamark, 2014).

The proteasome is the main degradation machinery of ubiquitinated proteins in normal growing conditions (Tomko and Hochstrasser, 2013). Proteasome-mediated protein degradation has one crucial difference from aggrephagy. Proteasomes preferentially degrade monomeric ubiquitinated proteins, whereas aggrephagy degrades multimeric ubiquitinated protein aggregates. In addition, inhibition of proteasome activity stimulates aggresome formation (Lamark and Johansen, 2010). These results suggest that proteasome and aggresome/aggrephagy have distinct roles but coordinative regulations to inactivate the cytotoxicities of ubiquitinated proteins.

¹Division of Virology, Niigata University Graduate School of Medical and Dental Sciences, Niigata 951-8510, Japan

²Department of Pathology, Brain Research Institute, Niigata University, Niigata 951-8585, Japan

³Electron Microscope Core Facility, Niigata University, Niigata 951-8510, Japan

⁴Department of Molecular Neurobiology, Brain Research Institute, Niigata University, Niigata 951-8510, Japan

⁵Department of Microbiology, Kanazawa Medical University School of Medicine, Uchinada, 920-0293, Japan

⁶Department of Biochemistry, Niigata University Graduate School of Medical and Dental Sciences, Niigata 951-8510, Japan

⁷Lead Contact

*Correspondence: fujiiimas@med.niigata-u.ac.jp
<https://doi.org/10.1016/j.isci.2018.11.006>



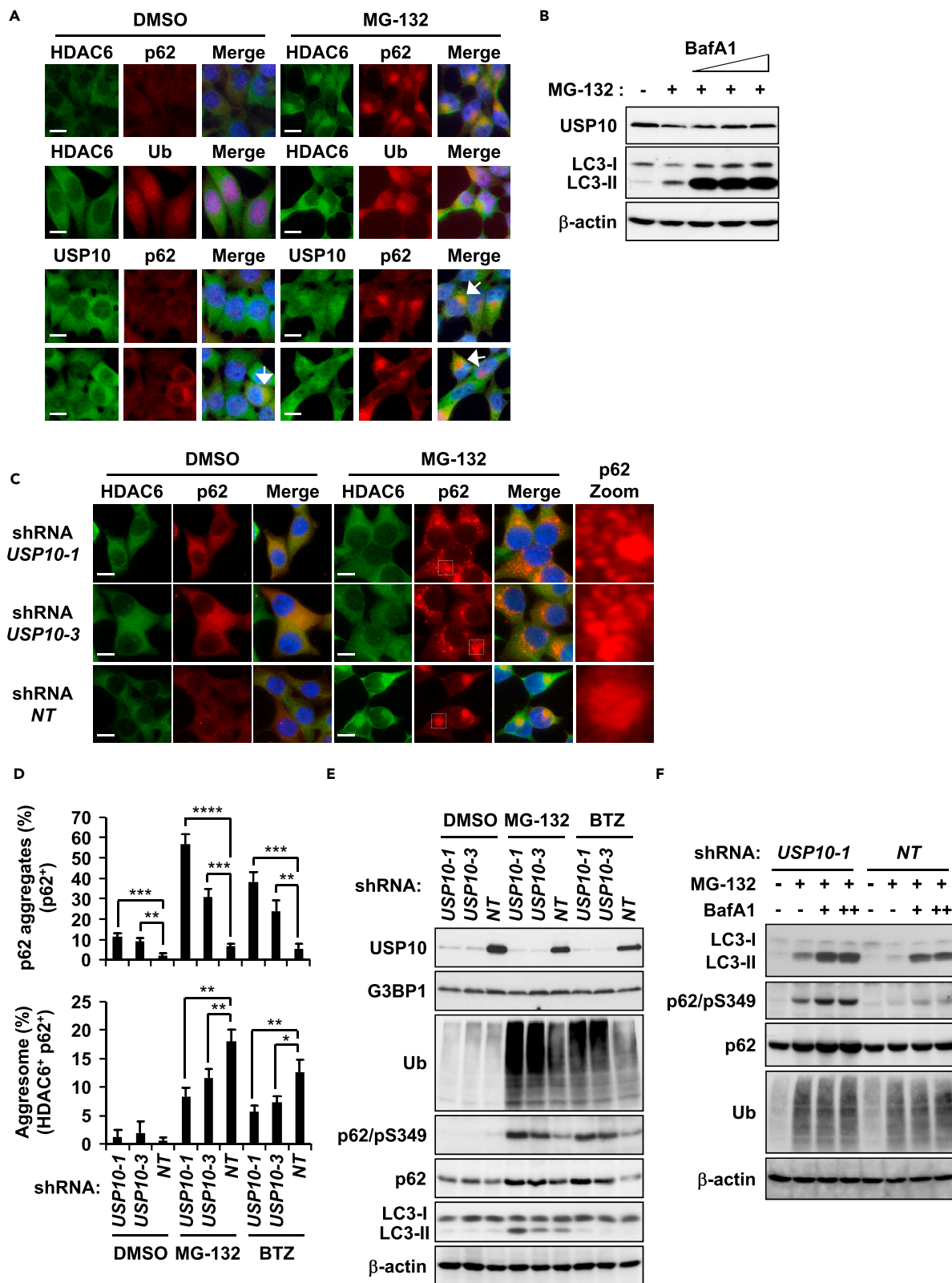


Figure 1. USP10 Knockdown Impairs Aggresome Formation

(A) HeLa cells were treated with 5 μ M MG-132 or DMSO for 12 hr, and the cells were stained with anti-HDAC6 (green) or anti-USP10 (green) antibody with either the anti-p62 (red) or anti-ubiquitin (Ub) (red) antibody. Nuclei were counterstained using Hoechst 33258 (blue). Arrows indicate cells with USP10/p62-double-positive aggregates. Scale bars, 10 μ m.

(B) HeLa cells were pretreated with 2.5, 5, and 10 nM bafilomycin A1 (BafA1) or DMSO for 0.5 hr and further treated with MG-132 or DMSO for 12 hr. The whole-cell extracts were characterized by western blot (WB) analysis using anti-USP10, anti-LC3, and anti- β -actin antibodies.

(C) USP10-KD (*USP10-1* or *USP10-3*) and control (NT) HeLa cells were treated with MG-132 or DMSO for 12 hr, and the cells were stained with anti-HDAC6 (green) and anti-p62 (red) antibodies and with Hoechst 33258 (blue). Scale bars, 10 μ m.

(D) The indicated HeLa cells were treated with MG-132, 1 μ M bortezomib (BTZ), or DMSO for 12 hr. Cells with one large HDAC6/p62-double-positive aggregate (more than 15 μ m² in size) at the perinuclear region with nuclear deformity were counted as aggresome-positive cells. Cells with multiple small HDAC6-negative/p62-positive aggregates (less than 10 μ m² in size) were counted as p62-aggregate-positive cells. The number of cells with p62 aggregates or aggresome are presented as the mean \pm SD ($n = 3$); * $p < 0.05$; ** $p < 0.01$; *** $p < 0.001$; **** $p < 0.0001$.

(E) Whole-cell extracts prepared from the indicated HeLa cells were characterized by WB using anti-USP10, anti-G3BP1, anti-Ub, anti-p62/pS349, anti-p62, anti-LC3, and anti- β -actin antibodies.

(F) The indicated HeLa cells were pretreated with increasing concentrations of BafA1 (–, DMSO; +, 5 nM BafA1; ++, 10 nM BafA1) and further treated with MG-132 or DMSO for 12 hr. The whole-cell extracts were characterized by WB using anti-LC3, anti-p62/pS349, anti-p62, anti-Ub, and anti- β -actin antibodies. See also Figure S1.

Ubiquitin-specific protease 10 (USP10) is a deubiquitinase that is ubiquitously expressed in many cell types, and a genetic knockout of *Usp10* in mice leads to bone marrow failure and death at an early age (Higuchi et al., 2016). Substrates of USP10 deubiquitinase include various stress regulators, the tumor suppressor p53 (Yuan et al., 2010), sirtuin6 (SIRT6) (Lin et al., 2013) and adenosine monophosphate-activated protein kinase (Deng et al., 2016). USP10 also has deubiquitinase-independent functions, such that USP10 inhibits apoptosis by reducing reactive oxygen species (ROS) production induced by an oxidative stress inducer arsenite (Takahashi et al., 2013b). These results suggest that USP10 is a critical stress-protective factor under various stress conditions.

In this study, we found that USP10 efficiently inactivates the cytotoxicities of ubiquitinated proteins by inducing aggresomes in a deubiquitinase-independent manner. Cystic fibrosis transmembrane conductance regulator (CFTR)- Δ F508 (Johnston et al., 1998), α -synuclein (Spillantini et al., 1997), and aminoacyl-tRNA synthetase complex-interacting multifunctional protein-2 (AIMP2) (Corti et al., 2003) are aggregation-prone proteins associated with the development of cystic fibrosis or PD. USP10 stimulated protein aggregation initiated by these proteins, thereby inducing aggresome formation. A proteasome reporter assay indicated that USP10 together with certain amounts of ubiquitination-prone proteins inhibits proteasome activity, which promoted protein aggregation and aggresome formation. To promote protein aggregation and aggresome formation, USP10 interacted with p62, and they cooperatively inhibited caspase-3-associated cell death. Importantly, USP10 was colocalized with α -synuclein of Lewy bodies in PD, and colocalization of USP10 and α -synuclein in Lewy bodies resembled those in aggresomes of cultured cells, suggesting that USP10 promotes Lewy body formation by an aggresome-related mechanism and inhibits neurotoxicities. Collectively, the present study showed that USP10 is a critical factor that inhibits cytotoxicities of ubiquitinated proteins in protein-aggregation-associated diseases by inducing aggresome formation.

RESULTS**USP10 Is Localized in Aggresomes**

HeLa cells were treated with proteasome inhibitor (PI) MG-132 for 12 hr to examine whether USP10 is localized in aggresomes. MG-132 treatment induced mostly one large (more than 15 μ m² in size) aggresome per cell, which was detected with four aggresome marker proteins (p62, HDAC6, ubiquitin, and proteasome subunit α type-3 [PSMA3]) at the perinuclear regions with nuclear deformity, and the p62-positive aggresome was colocalized with USP10 (Figures 1A and S1A). In addition, MG-132 treatment of primary-neuron-enriched cells prepared from rat cortical tissues induced one large HDAC6/p62-positive aggresome with nuclear deformity, and p62-positive aggresomes colocalized with USP10 (Figure S1B). Approximately 90% of these primary cells consisted of MAP2-positive neurons (data not shown).

Aggresomes are tightly linked to lysosome-mediated degradation of aggresome-localized proteins. We examined the interaction of aggresomes with lysosomes using a lysosome marker protein, lysosome-associated membrane protein-1 (LAMP-1). One LAMP-1-positive aggregate per aggresome was always detected (Figure S1C).

We next examined whether USP10 is degraded by autophagy. Bafilomycin A1 (BafA1) is an inhibitor of autophagosome fusion with lysosomes, and the cotreatment of MG-132 with BafA1 increased the amount of the autophagy substrate LC3-II (Figure 1B). MG-132 treatment reduced the amount of USP10, and the reduction is attenuated by cotreatment with BafA1 (Figure 1B), indicating that USP10 is degraded by autophagy.

Knockdown of USP10 Reduces Aggresome Formation and Induces Many p62-Positive Aggregates

We next examined whether USP10 plays a role in aggresome formation in HeLa cells by RNA-interference-mediated knockdown of USP10 (USP10-KD). After treatment of HeLa cells with PI, USP10-KD reduced the number of cells with p62/HDAC6-double-positive aggresomes at the perinuclear region, whereas USP10-KD induced multiple p62-positive/HDAC6-negative aggregates throughout the cytoplasm (Figures 1C and 1D). USP10-KD also reduced aggresome formation in the 293T embryonic kidney cell line (Figures S1D–S1F).

Western blot analysis showed that treatment of wild-type USP10 (USP10-WT) cells with PI increased the amounts of ubiquitinated proteins and phosphorylated p62 at Ser349 (p62/pS349) (Figure 1E). p62/pS349 increases the interaction of p62 with Keap1, an interaction that reduces ubiquitin-dependent degradation of transcription factor Nrf2 and stimulates Nrf2-dependent transcriptional activation of antioxidant genes such as NAD(P)H dehydrogenase quinone 1 (Nqo1) (Ichimura et al., 2013). MG-132-treated USP10-KD cells expressed p62, p62/pS349, ubiquitinated proteins, and LC3-II more than USP10-WT cells (Figure 1E), and the amounts of p62, p62/pS349, and LC3-II in USP10-KD cells were further augmented by cotreatment with BafA1 (Figure 1F). These results suggested that USP10-KD reduces aggresome formation but does not inhibit the autophagy degradation of p62, p62/pS349, and LC3-II.

LC3/p62 aggregates are used as markers of autophagosomes and/or autolysosomes (autophagosomes fused with lysosomes) (Pankiv et al., 2007). LC3/p62-positive aggregates were weakly detected in USP10-KD and USP10-WT cells with or without MG-132 treatment, whereas LC3/p62-positive aggregates were prominently induced by BafA1 treatment with or without MG-132 treatment (Figure S1G). These results suggested that LC3 is degraded by autophagy in both USP10-WT and USP10-KD cells with or without MG-132 treatment, and that USP10-KD does not inhibit autophagy-mediated degradation of LC3. Noteworthy, BafA1 treatment inhibited MG-132-induced aggresome formation, whereas it induced the formation of p62/LC3-double-positive/HDAC6-negative aggregates, which resembled that observed in MG-132-treated USP10-KD cells (Figure S1G). These results suggested that the fusion of p62/LC3-positive autophagosomes with lysosomes promotes aggresome formation.

USP10 Augments Aggresome Formation by Increasing the Amount of Ubiquitinated Proteins

We next examined the activity of USP10 toward ubiquitinated protein aggregation. Cystic fibrosis is an inherited genetic disease caused by mutations of the CFTR gene (Cheng et al., 1990). CFTR-ΔF508 is a pathogenic CFTR mutant with a single amino acid deletion and is aggregation-prone (Lukacs and Verkman, 2012). Expression of GFP-tagged CFTR-ΔF508 (GFP-CFTR-ΔF508) in HeLa cells formed aggresome-like structures containing CFTR-ΔF508, and these structures were augmented by MG-132 but not BafA1, and the augmentation was accompanied by an increase in the amount of CFTR-ΔF508 (Figures 2A and 2B). Since these CFTR-ΔF508-induced aggregates were stained with aggresome marker proteins, HDAC6, p62, and ubiquitin (Figures 2A and S2A), we refer to these CFTR-ΔF508-induced aggregates as CFTR-ΔF508-induced aggresomes in the following section. ProteoStat dye visualizes misfolded protein aggregates, and staining is a marker of aggresomes (Shen et al., 2011). CFTR-ΔF508-induced aggresomes were stained with ProteoStat, suggesting that CFTR-ΔF508-induced aggresomes contain misfolded protein aggregates (Figure S2A). Coexpression of USP10 without MG-132 also promoted CFTR-ΔF508-induced aggresome formation and increased the amount of CFTR-ΔF508 (Figures 2B and S2B). In contrast, USP10-KD reduced aggresome formation of CFTR-ΔF508 and the amount of CFTR-ΔF508, and the reductions were partially rescued by exogenous USP10 (Figure 2C). Fractionation of cell lysates by a detergent showed that coexpression of USP10 with CFTR-ΔF508 predominantly increases the amounts of detergent-insoluble CFTR-ΔF508 as well as the amounts of soluble and insoluble ubiquitinated proteins (Figure 2D). These results indicate that USP10 augments CFTR-ΔF508-induced aggresome formation, and augmentation was mediated partly by increasing the amounts of CFTR-ΔF508 and ubiquitinated proteins.

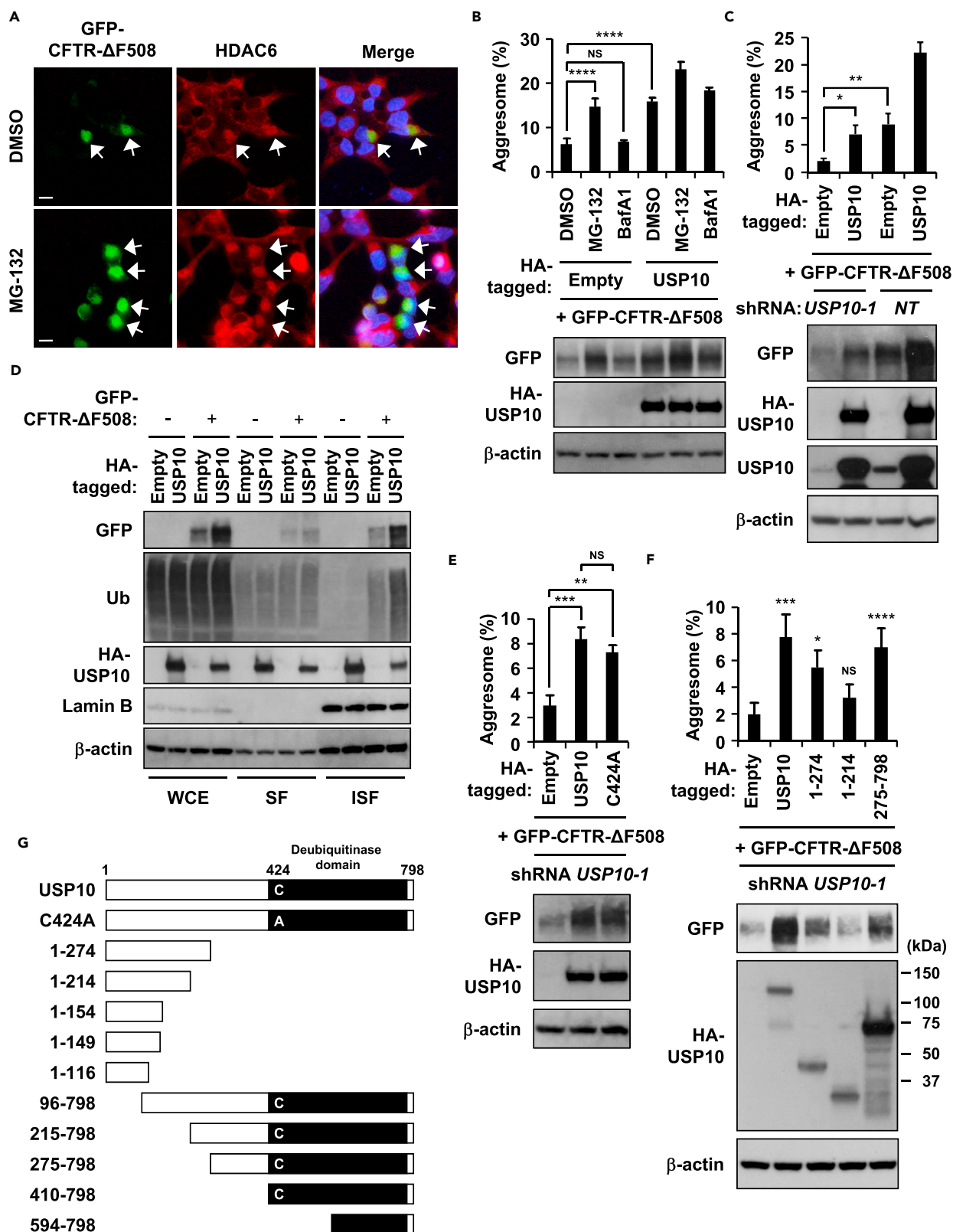


Figure 2. Overexpression of USP10 Stimulates Aggresome Formation

(A) HeLa cells were transfected with the GFP-CFTR- Δ F508 plasmid and treated with 5 μ M MG-132 or DMSO for 12 hr. The cells were stained with the anti-HDAC6 antibody (red) and Hoechst 33258 (blue). Arrows indicate localizations of HDAC6 at CFTR- Δ F508-induced aggresomes. Scale bars, 10 μ m.

(B) HeLa cells were transfected with the HA-tagged USP10 (HA-USP10) and GFP-CFTR- Δ F508 plasmids, and the cells were treated with MG-132, 10 nM BafA1, or DMSO for 6 hr. Cells with GFP/HDAC6-double-positive aggresomes (more than 15 μ m² in size) at the perinuclear region with nuclear deformity were counted as aggresome-positive cells. The percentages of cells with GFP-positive aggresome are presented as the mean \pm SD ($n = 3$); **** $p < 0.0001$; NS, not significant. Simultaneously, whole-cell extracts were characterized by western blot (WB) using anti-GFP, anti-HA, and anti- β -actin antibodies.

(C) USP10-KD (*USP10-1*) and control (NT) HeLa cells were transfected with the HA-USP10 and the GFP-CFTR- Δ F508 plasmids. The percentages of cells with GFP/HDAC6-positive aggresome are presented as the mean \pm SD ($n = 3$); * $p < 0.05$; ** $p < 0.01$. Simultaneously, whole-cell extracts were characterized by WB using anti-GFP, anti-HA, anti-USP10, and anti- β -actin antibodies.

(D) HeLa cells were transfected with the HA-USP10 plasmid with or without the GFP-CFTR- Δ F508 plasmid, and the whole-cell extracts (WCE), NP-40-soluble fractions (SF), and NP-40-insoluble fractions (ISF) were characterized by WB using anti-GFP, anti-Ub, anti-HA, anti-Lamin B, and anti- β -actin antibodies.

(E) USP10-KD (*USP10-1*) HeLa cells were transfected with HA-USP10 or its deubiquitinase-inactive mutant USP10^{C424A} plasmid together with the GFP-CFTR- Δ F508 plasmid. The percentages of cells with GFP/HDAC6-positive aggresome are presented as mean \pm SD ($n = 4$); ** $p < 0.01$; *** $p < 0.001$; NS, not significant. Simultaneously, whole-cell extracts were characterized by WB using anti-GFP, anti-HA, and anti- β -actin antibodies.

(F) USP10-KD (*USP10-1*) HeLa cells were transfected with HA-USP10 or its mutant (USP10¹⁻²⁷⁴, USP10¹⁻²¹⁴, or USP10²⁷⁵⁻⁷⁹⁸) plasmid together with the GFP-CFTR- Δ F508 plasmid. The percentages of cells with GFP/HDAC6-positive aggresome are presented as the mean \pm SD ($n = 4$); * $p < 0.05$; *** $p < 0.001$; **** $p < 0.0001$; NS, not significant. Simultaneously, whole-cell extracts were characterized by WB using anti-GFP, anti-HA, and anti- β -actin antibodies.

(G) Schematic representation of human USP10 mutants used in this study.
See also [Figure S2](#).

To delineate the USP10 activity to aggresome formation, we characterized several USP10 mutants in USP10-KD cells. USP10^{C424A} is inactive in deubiquitinating activity (Yuan et al., 2010). We confirmed that wild-type USP10 but not USP10^{C424A} deubiquitinates the p53 protein (Figure S2C). USP10^{C424A} showed almost equivalent aggresome-augmenting activity to wild-type USP10 (USP10-WT), suggesting that the deubiquitinating activity of USP10 is not required for the aggresome-augmenting activity of USP10 (Figures 2E and S2D). USP10¹⁻²⁷⁴ and USP10²⁷⁵⁻⁷⁹⁸ but not USP10¹⁻²¹⁴ increased the amount of CFTR- Δ F508 and simultaneously augmented aggresome formation (Figures 2F and 2G). These results suggested that both N- and C-terminal regions of USP10 are critical for maximizing aggresome-augmenting activity of USP10 to CFTR- Δ F508.

The generality of USP10 activity to protein aggregation was explored by examining the activity of USP10 to two additional aggregation-prone proteins, α -synuclein and AIMP2. Both α -synuclein and AIMP2 are associated with PD and are components of inclusions called Lewy bodies in brain lesions (Ko et al., 2005; Spillantini et al., 1997). Synphilin-1 is an interactor of α -synuclein, and is often coexpressed with α -synuclein to induce protein aggregation (Engelender et al., 1999). GFP-tagged α -synuclein (GFP- α -synuclein) and hemagglutinin (HA)-tagged AIMP2 (HA-AIMP2) were localized in aggresomes of HeLa cells treated with MG-132 (Figures S3A and S3B). Coexpression of USP10 with either α -synuclein or AIMP2 without MG-132 augmented the number of aggresome-like aggregates containing α -synuclein and AIMP2, respectively (Figures 3A, 3B, S3C, and S3D). USP10 was often localized at the periphery of α -synuclein- or AIMP2-induced aggresomes (Figures S3C and S3E). We also often detected localization of USP10 at the periphery of aggresomes containing endogenous α -synuclein in neuronal Neuro-2a cells (Figure 3C). Noteworthy, expression of α -synuclein without USP10 overexpression induced HDAC6/p62/ubiquitin-negative aggregates that were distinct from α -synuclein-/USP10-induced aggresome-like aggregates and these aggregates were colocalized with endogenous USP10 (Figure S3C).

Like CFTR- Δ F508, coexpression of USP10 with GFP- α -synuclein and synphilin-1 increased the amounts of insoluble α -synuclein and insoluble ubiquitinated proteins (Figure 3D). USP10 also increased the amount of non-tagged α -synuclein (Figure S3F). Coexpression of USP10 with AIMP2 slightly increased the amount of ubiquitinated proteins, but the increases were much smaller than those caused by the coexpression of USP10 with CFTR- Δ F508 (Figure 3D). As AIMP2 without coexpression of USP10 highly increased the amount of ubiquitinated proteins (Figure 3D), we assumed that endogenous USP10 is sufficient for AIMP2-mediated increase of ubiquitinated proteins. Indeed, USP10-KD dramatically reduced an AIMP2-mediated increase of ubiquitinated proteins and this reduction was rescued by the expression of exogenous USP10 (Figure 3E). These results indicated that USP10 increases the amounts of ubiquitinated proteins induced by overexpression of several aggregation-prone proteins, thereby promoting aggresome formation.

Based on USP10-induced ubiquitinated protein aggregation, we hypothesized that coexpression of USP10 with an aggregation-prone protein inhibits proteasome activity. To examine this possibility, we measured

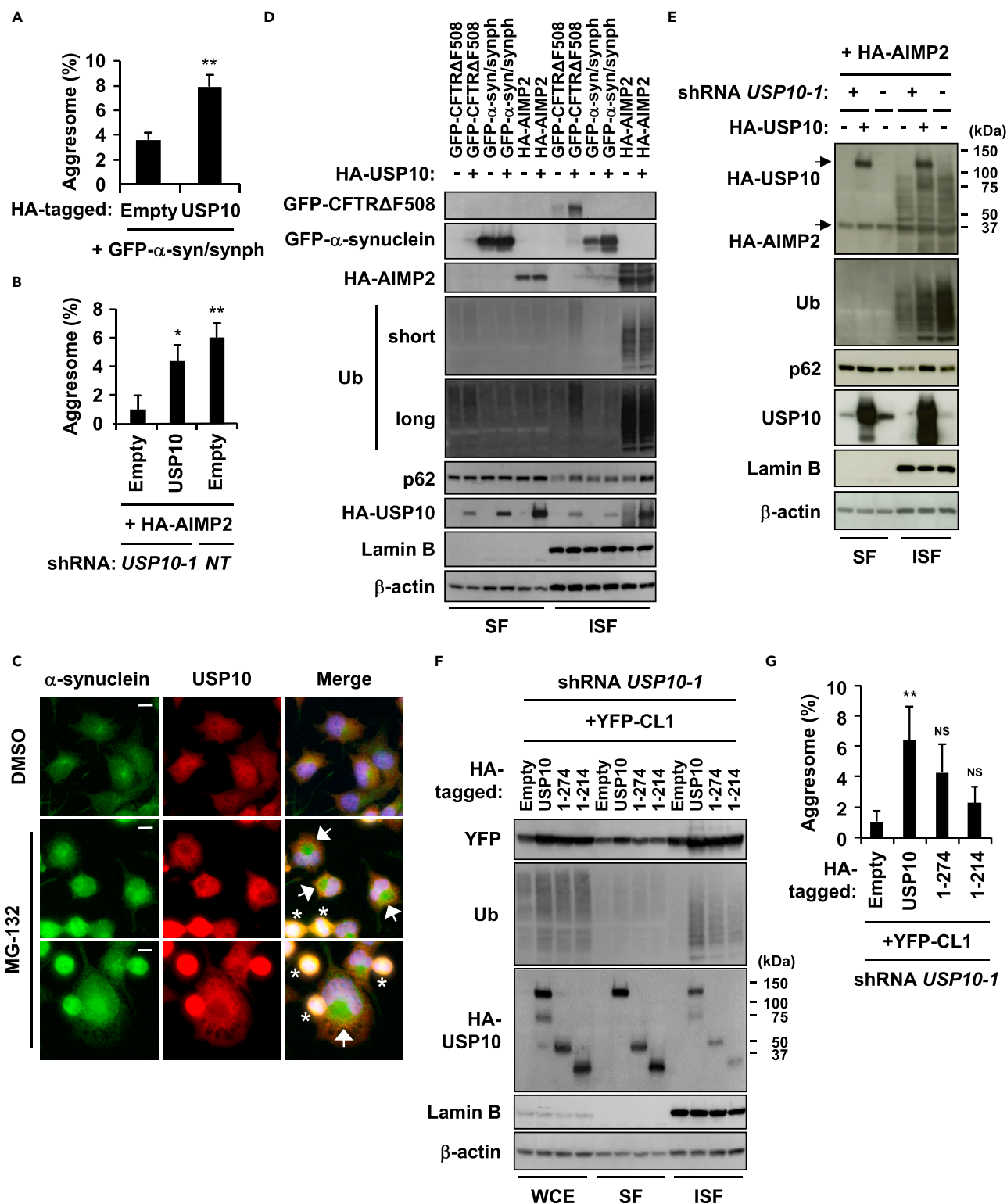


Figure 3. USP10 Increases the Amount of Insoluble Ubiquitinated Proteins

(A) HeLa cells were transfected with HA-USP10, GFP- α -synuclein (GFP- α -syn), and Myc-synphilin-1 (synph) plasmids. The percentages of cells with GFP/USP10-positive aggresome are presented as the mean \pm SD (n = 3); **p < 0.01.

Figure 3. Continued

(B) USP10-KD (*USP10-1*) and control (*NT*) HeLa cells were transfected with the non-tagged USP10 and the HA-AIMP2 plasmids. The percentages of cells with HA/USP10-positive aggresomes are presented as the mean \pm SD ($n = 3$); * $p < 0.05$; ** $p < 0.01$.

(C) Neuro-2a cells were treated with 0.5 μ M MG-132 or DMSO for 12 hr. The cells were stained with the anti- α -synuclein (green) and anti-USP10 (red) antibodies and with Hoechst 33258 (blue). Arrows indicate α -synuclein-positive aggresomes induced by MG-132. Asterisks indicate dead cells. Scale bars, 10 μ m.

(D) HeLa cells were transfected with the HA-USP10, the GFP-CFTR- Δ F508, GFP- α -syn/synph, or the HA-AIMP2 plasmid, and NP-40-soluble fractions (SF) and NP40-insoluble fractions (ISF) were characterized by western blot (WB) using anti-GFP, anti-HA, anti-Ub, anti-p62, anti-Lamin B, and anti- β -actin antibodies.

(E) USP10-KD (*USP10-1*) and control (*NT*) HeLa cells were transfected with the HA-USP10 and the HA-AIMP2 plasmids, and SF and ISF were characterized by WB using anti-HA, anti-Ub, anti-p62, anti-USP10, anti-Lamin B, and anti- β -actin antibodies.

(F) USP10-KD (*USP10-1*) HeLa cells were transfected with HA-USP10 or its mutant (*USP10¹⁻²⁷⁴* or *USP10¹⁻²¹⁴*) plasmid together with the YFP-CL1 plasmid, and whole-cell extracts (WCE), SF, and ISF were characterized by WB using anti-GFP, anti-Ub, anti-HA, anti-Lamin B, and anti- β -actin antibodies.

(G) The percentages of cells with YFP/HDAC6-positive aggresome are presented as the mean \pm SD ($n = 4$); ** $p < 0.01$; NS: not significant.

See also [Figure S3](#).

proteasome activity by using CL1. CL1 is the 16-amino-acid polypeptide containing an ubiquitination-prone site ([Gilon et al., 1998](#)). YFP-CL1 is a fusion protein of CL1 with yellow fluorescent protein (YFP), and it is degraded by proteasomes. Thus, YFP-CL1 is used as a reporter to measure proteasome activity ([Menendez-Benito et al., 2005](#)). Coexpression of USP10 with YFP-CL1 increased the amounts of insoluble YFP-CL1 and insoluble ubiquitinated proteins ([Figure 3F](#)). These results suggested that coexpression of USP10 with an aggregation-prone protein inhibits proteasome activity to increase the amount of insoluble ubiquitinated proteins, thereby augmenting aggresome formation. Like CFTR- Δ F508, the aggregation-inducing activities of USP10-WT toward YFP-CL1 was higher than those of *USP10¹⁻²⁷⁴* and *USP10¹⁻²¹⁴* ([Figure 3G](#)).

USP10 Promotes Aggresome Formation by Interacting with p62

p62 is a ubiquitin-binding protein and plays a critical role in ubiquitinated protein aggregation ([Komatsu et al., 2007](#)). Thus, we examined whether USP10 interacts with p62. The immunoprecipitation assay indicated that endogenous p62 interacted with endogenous USP10 together with previously known p62 interactors HDAC6 or dynein ([Calderilla-Barbosa et al., 2014](#); [Yan et al., 2013](#)), both of which are important for aggresome formation ([Figure 4A](#)). In contrast, the interaction of USP10 with CFTR- Δ F508 could not be detected ([Figure 4B](#)). Co-immunoprecipitation of USP10 deletion mutants with p62 indicated that both N- and C-terminal regions of USP10, *USP10¹⁻²⁷⁴*, and *USP10²⁷⁵⁻⁷⁹⁸*, but not *USP10¹⁻²¹⁴*, interact with p62 ([Figures 4C–4E](#) and [2G](#)). As *USP10¹⁻²⁷⁴* and *USP10²⁷⁵⁻⁷⁹⁸*, but not *USP10¹⁻²¹⁴*, promoted aggresome formation induced by CFTR- Δ F508 ([Figure 2F](#)), these results suggested that USP10 promotes aggresome formation by interacting with p62.

To investigate whether p62 plays a positive role in USP10-induced protein aggregation, we examined CFTR- Δ F508-induced protein aggregation in p62-KD cells. p62-KD reduced the amounts of insoluble CFTR- Δ F508, insoluble ubiquitinated proteins, and insoluble USP10 induced by CFTR- Δ F508/USP10, and simultaneously reduced aggresome formation ([Figures 5A](#) and [5B](#)). Moreover, USP10 expression increased the amount of insoluble p62 in p62 wild-type cells ([Figure 5B](#)). Collectively, these results indicated that USP10 induces ubiquitinated protein aggregation and aggresome formation, and this is facilitated partly by interacting with p62.

Conversely, we examined the role of USP10 in p62-induced protein aggregation. Overexpression of p62 in HeLa cells without MG-132-treatment induced large and small p62-positive aggregates ([Figure 5C](#)). Large p62-positive aggregates were colocalized with ubiquitin, HDAC6, USP10, and GFP-LC3 (LC3 fusion protein of GFP), and therefore resembled aggresomes ([Figures 5C](#) and [5D](#)). In contrast, small p62 aggregates were colocalized with ubiquitin and GFP-LC3, but not with USP10 ([Figures 5C](#) and [5D](#)), and these aggregates resembled p62 aggregates in USP10-KD cells treated with MG-132 ([Figure 1C](#)). Coexpression of USP10 with p62 augmented the sizes of p62-induced aggregates/aggresomes ([Figures 5E](#) and [5F](#)). These results suggested that USP10 converts small USP10-negative p62 aggregates to USP10/p62-double-positive aggregates/aggresomes. In addition to USP10-WT, *USP10⁹⁶⁻⁷⁹⁸*, but not *USP10¹⁻¹¹⁶*, increased the size of p62 aggregates/aggresomes ([Figures 5E](#) and [5F](#)). Given that *USP10⁹⁶⁻⁷⁹⁸* but not *USP10¹⁻²¹⁴* interacts with p62 ([Figures 4C](#) and [4D](#)), these results also suggested that USP10 interaction with p62 induces large p62 aggregates/aggresomes. *USP10^{C424A}* increased the size of p62-induced aggresomes equivalently to USP10-WT ([Figures 5E](#) and [5F](#)), suggesting that the deubiquitinating activity of USP10 is not required for the augmentation of p62-induced aggregation.

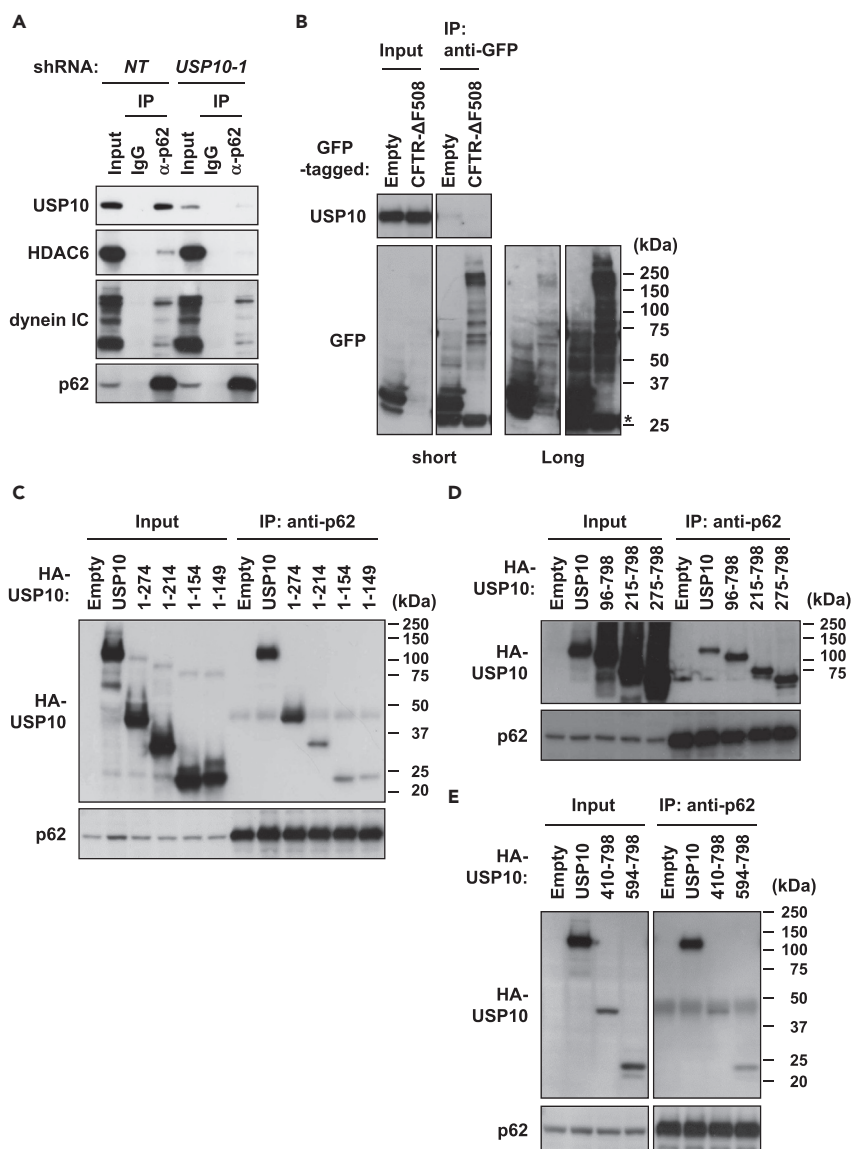


Figure 4. p62 Interacts with USP10

(A) Cell lysates prepared from control (NT) and USP10-KD (*USP10-1*) HeLa cells were immunoprecipitated with the anti-p62 antibody or normal rabbit IgG. The cell lysate (Input) and immunoprecipitates (IP) were characterized by western blot (WB) with anti-USP10, anti-HDAC6, anti-dynein intermediate chain (IC), and anti-p62 antibodies.

(B) HeLa cells were transfected with the GFP-CFTR- Δ F508 plasmid or empty control. Cell lysates (Input) and immunoprecipitates with the anti-GFP antibody (IP) were characterized by WB using anti-USP10 and anti-GFP antibodies. The asterisk indicates a nonspecific band.

(C–E) HeLa cells were transfected with HA-USP10 or its mutant ($USP10^{1-274}$, $USP10^{1-214}$, $USP10^{1-154}$, or $USP10^{1-149}$ in C; $USP10^{96-798}$, $USP10^{215-798}$, or $USP10^{275-798}$ in D; and $USP10^{410-798}$ or $USP10^{594-798}$ in E) plasmid. Cell lysates (Input) and immunoprecipitates with the anti-p62 antibody (IP) were characterized by WB with anti-HA and anti-p62 antibodies.

USP10 showed two opposite activities to the amounts of p62 and ubiquitinated proteins in cells either treated or not treated with MG-132 (Figures 5B and 1E). USP10 overexpression without MG-132 treatment increased the amounts of p62 and insoluble ubiquitinated proteins (Figure 5B), whereas USP10-KD cells treated with MG-132 increased the amounts of p62 and ubiquitinated proteins more than USP10-WT cells (Figure 1E). We showed previously that USP10-KD increases the production of ROS by an oxidant (arsenite) (Takahashi et al., 2013a). The different USP10 activities might be explained by the production of ROS stimulated by MG-132 treatment. Since ROS increases the expression of p62 by activating transcription factor

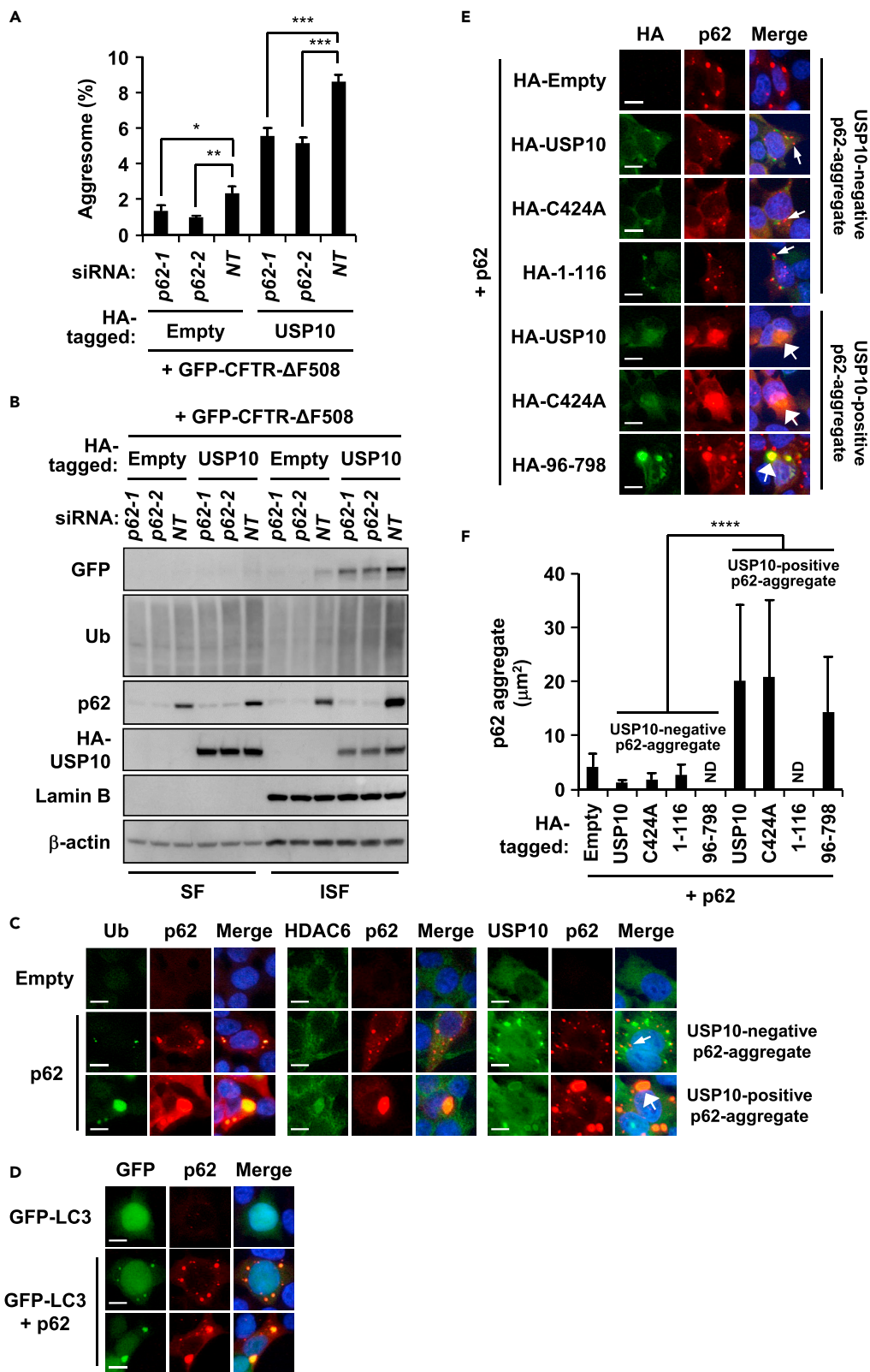


Figure 5. p62 Mediates USP10-Induced Protein Aggregation

(A) HeLa cells were transfected with p62 small interfering RNA (siRNA) (p62-1 or p62-2) or control siRNA (NT) and were further transfected with the HA-USP10 and the GFP-CFTR- Δ F508 plasmids. The percentages of cells with GFP/HDAC6-positive aggresome are presented as the mean \pm SD ($n = 4$); * $p < 0.05$; ** $p < 0.01$; *** $p < 0.001$.

(B) The NP-40-soluble fractions (SF) and NP-40-insoluble fractions (ISF) from the indicated HeLa cells were characterized by western blot (WB) using anti-GFP, anti-Ub, anti-p62, anti-HA, anti-Lamin B, and anti- β -actin antibodies.

(C) HeLa cells were transfected with the p62 plasmid. The cells were stained with the anti-p62 (red) antibody and with anti-Ub (green), anti-HDAC6 (green), or anti-USP10 (green) antibody, and with Hoechst 33258 (blue). The small arrow indicates USP10-negative p62 aggregate, whereas the large arrow indicates USP10-positive p62 aggregate. Scale bars, 10 μ m.

(D) HeLa cells were transfected with the p62 and the GFP-LC3 plasmids. The cells were stained with the anti-p62 antibody (red) and Hoechst 33258 (blue). Scale bars, 10 μ m.

(E) HeLa cells were transfected with the p62 plasmid and HA-USP10 or its mutant plasmids (USP10^{C424A}, USP10¹⁻¹¹⁶, or USP10⁹⁶⁻⁷⁹⁸). The cells were stained with anti-HA (green) and anti-p62 (red) antibodies, and with Hoechst 33258 (blue). Small arrows indicate HA-USP10-negative p62 aggregates, whereas the large arrows indicate HA-USP10-positive p62 aggregates. Scale bars, 10 μ m.

(F) The sizes of p62 aggregates (μ m²) are presented as the mean \pm SD ($n = 30$); **** $p < 0.0001$; ND, not detected.

See also Figure S4.

Nrf2 (Jain et al., 2010; Jaramillo and Zhang, 2013), ROS produced in MG-132-treated USP10-KD cells might induce p62 and ubiquitinated proteins more than USP10-WT cells. USP10-KD cells treated with MG-132 possessed more ROS and nuclear Nrf2 than USP10-WT cells, and cells with high nuclear Nrf2 induced more p62 protein (Figures S4A–S4C). In addition, an antioxidant N-acetylcysteine reduced the amount of p62 aggregates in USP10-KD cells treated with PI (Figure S4D). These results suggested that MG-132 treatment stimulates ROS production more in USP10-KD cells than in USP10-WT cells, and such ROS then induce nuclear activated Nrf2 in USP10-KD cells, thereby increasing the amounts of p62 and ubiquitinated proteins. These results suggested that USP10 has two opposing activities to p62-dependent protein aggregation that are dependent on the level of ROS.

USP10 Inhibits Cell Death Induced by MG-132

MG-132 induces cell death of cultured cells, and the death of these cells is inhibited by aggresome formation (Kawaguchi et al., 2003; Tanaka et al., 2004). Thus, we examined whether USP10 inhibits MG-132-induced cell death by measuring activated caspase-3 (cleaved caspase-3). An anti-cleaved caspase-3 antibody detected cell death of USP10-KD cells treated with MG-132, and the level was more than that of USP10-WT cells (Figures 6A and 6B). Interestingly, USP10-KD cells with p62 aggregates were more resistant to PI-induced cell death than cells without p62 aggregates, suggesting that p62 aggregates inhibit cell death induced by PI (Figure 6C).

To further examine the role of p62 in PI-induced cell death, we examined the sensitivity of p62-KD cells to PI. Nuclear condensation analysis showed that MG-132-induced cell death was augmented by either p62-KD or USP10-KD, and the level was further increased by their double-knockdowns (Figures 6D–6F). These results indicated that USP10 and p62 cooperatively inhibit MG-132-induced cell death by promoting the formation of aggresomes and p62 aggregates.

To obtain information describing how USP10 inhibits MG-132-induced cell death, we measured cell death of USP10-KD cells expressing several USP10 mutants. USP10-KD cells expressing USP10-WT were resistant to cell death induced by MG-132 more than cells without USP10-WT (Figures 6G, S5A, and S5B). USP10^{C424A} and USP10⁹⁶⁻⁷⁹⁸, but not USP10¹⁻²¹⁴, reduced cell death of USP10-KD cells (Figures 6G and S5A–S5C). Given that USP10-WT, USP10^{C424A}, and USP10⁹⁶⁻⁷⁹⁸, but not USP10¹⁻²¹⁴, in USP10-KD cells promoted p62 aggregation and aggresome formation (Figures 6G and S5A–S5C), these results suggested that USP10 inhibits cell death induced by MG-132 by promoting aggresome formation and p62 aggregation.

PD, a representative neurodegenerative disorder of synucleinopathy, always bears many α -synuclein-positive neuronal inclusions, namely, Lewy bodies (Peng et al., 2017). We found characteristic USP10 immunoreactivity in Lewy bodies in neurons of the substantia nigra, locus coeruleus, and other brain stem nuclei, where the halo and core of the inclusions were positive and negative, respectively (Figures 7A, 7B, 7F, and 7G and Table S1). A double-labeling immunofluorescent study demonstrated colocalization of phosphorylated α -synuclein and USP10 in Lewy bodies (Figures 7K, 7L, 7N, and 7O), indicating the possible association of both proteins. In contrast, in neurons of the controls and patients with PD without Lewy bodies, the reactivity was diffuse within the cytoplasm (Figures 7C and 7H). These results suggested that USP10 is involved in Lewy body formation.

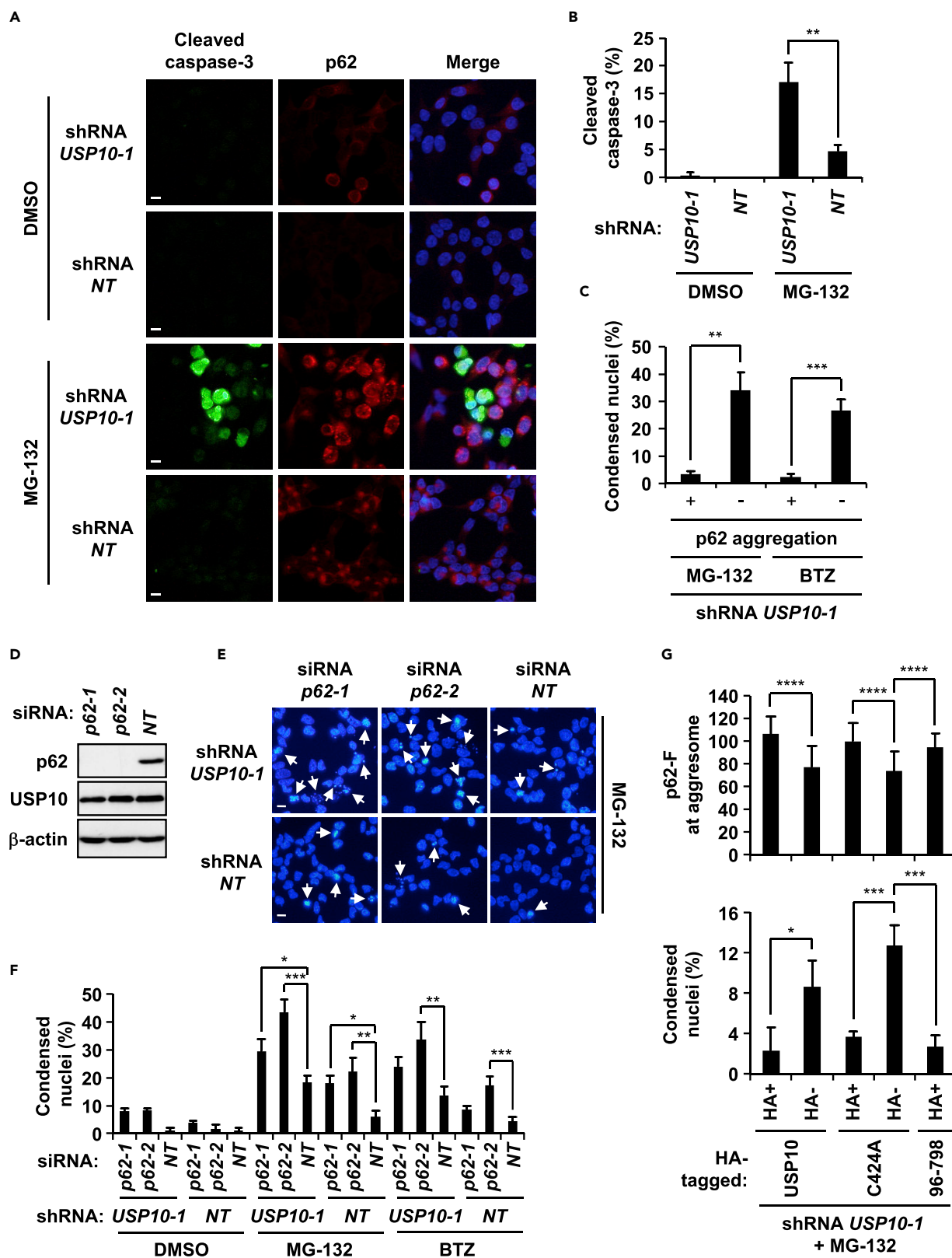


Figure 6. USP10 Knockdown Augments Cell Death Induced by a Proteasome Inhibitor

(A) USP10-KD (*USP10-1*) and control (*NT*) HeLa cells were treated with 5 μ M MG-132 or DMSO for 12 hr, and the cells were stained with anti-cleaved caspase-3 (green) and anti-p62 (red) antibodies, and with Hoechst 33258 (blue). Scale bars, 10 μ m.

(B) Apoptotic cells were assessed by staining cleaved caspase-3. Proportions of cleaved caspase-3-positive cells in USP10-KD (*USP10-1*) and control (*NT*) HeLa cells are presented as the mean \pm SD ($n = 3$); ** $p < 0.01$.

(C) USP10-KD (*USP10-1*) HeLa cells were treated with MG-132 or 1 μ M bortezomib (BTZ) for 12 hr, and the cells were stained with the anti-p62 antibody and Hoechst 33258. Proportions of cells containing condensed nuclei with or without p62 aggregates are presented as the mean \pm SD ($n = 3$); ** $p < 0.01$; *** $p < 0.001$.

(D) HeLa cells were transfected with p62 small interfering RNA (siRNA) (*p62-1* or *p62-2*) or control siRNA (*NT*) and cultured for 48 hr. Whole-cell extracts were characterized using western blot with anti-p62, anti-USP10, and anti- β -actin antibodies.

(E) USP10-KD (*USP10-1*) and control (*NT*) HeLa cells were transfected with p62 siRNA (*p62-1* or *p62-2*) or control siRNA (*NT*), and further treated with MG-132 for 12 hr. Cells were stained with Hoechst 33258 (blue). The arrows indicate cells containing condensed nuclei (apoptotic cells). Scale bars, 10 μ m.

(F) Proportions of cells containing condensed nuclei (apoptotic cells) are presented as the mean \pm SD ($n = 3$); * $p < 0.05$; ** $p < 0.01$; *** $p < 0.001$.

(G) p62 fluorescence at aggresome (more than 15 μ m² in size) (p62-F at aggresome; $n = 40$) or the proportions of condensed nuclei (condensed nuclei [%]; $n = 3$) in USP10-KD (*USP10-1*) HeLa cells expressing wild-type USP10, USP10^{C424A}, or USP10^{96–798} from Figures S5A or S5B are presented as the mean \pm SD; * $p < 0.05$; *** $p < 0.001$; **** $p < 0.0001$.

See also Figure S5.

We also examined USP10 immunoreactivity for oligodendroglial cytoplasmic inclusions (GCIs) in multiple system atrophy (MSA) (Figures 7D and 7I and Table S1), another representative disorder of synucleinopathy (Ahmed et al., 2012). We found no reactivity of anti-USP10 toward GCIs and oligodendrocytes in MSA and control samples (Figures 7D and 7I). Therefore, involvement of USP10 seems characteristic for Lewy bodies, rather than a common phenomenon in α -synuclein-containing inclusions.

Finally, we measured the amounts of α -synuclein, USP10, and aggresome-related proteins in brain (amygdala) lesions of patients with PD after separating the samples into Triton X-100-soluble and Triton X-100-insoluble fractions (Figure 8A and Table S2). Western blot analysis showed that the three patients with PD expressed more phosphorylated α -synuclein, α -synuclein, and synphilin-1 in the detergent-insoluble fraction than the two control samples. These results are consistent with the fact that phosphorylated α -synuclein is the major component of Lewy bodies in patients with PD (Anderson et al., 2006). Patients with PD also expressed soluble and/or insoluble USP10 proteins more than the controls. In addition, the amount of aggresome-inducing protein HDAC6 in the soluble fraction was increased in PD samples relative to the control samples. These results support the notion that USP10 and aggresomes play a role in Lewy body formation (Figure 8B).

DISCUSSION

Ubiquitinated proteins generated under various stress conditions, such as oxidative stress and proteasome dysfunction, are cytotoxic. To inactivate these cytotoxicities, cells induce aggresomes to promote cell survival. In this study, we found that USP10 is an essential factor to inactivate cytotoxicities of ubiquitinated proteins by inducing aggresome formation.

We showed that USP10 promotes aggresome formation partly by inhibiting the proteasome-mediated degradation of ubiquitinated proteins. The CFTR- Δ F508 protein was degraded by proteasomes in HeLa cells (Figure 2B), and coexpression with USP10 increased the amount of insoluble ubiquitinated proteins, including CFTR- Δ F508 by itself, which promoted aggresome formation (Figures 2B and 2D). Such USP10 activity was also detected with two other ubiquitination-prone proteins, α -synuclein and AIMP2 (Figures 3A, 3B, 3D, and 3E). Moreover, a proteasome activity reporter YFP-CL1 indicated that USP10 together with YFP-CL1 inhibits proteasome activity (Figure 3F). These results are consistent with previous studies showing that protein aggregates inhibit proteasome activity (Hipp et al., 2014). The proteasome enzyme subunit PSMA3 was also detected in both MG-132-induced and USP10-induced aggresomes (Figures S1A and S2E). Moreover, p62 has been shown to interact with ubiquitinated proteasome components (Cohen-Kaplan et al., 2016). Thus, USP10 and p62 might inhibit proteasome activity by trapping proteasome components in protein aggregates and/or aggresomes.

Interaction of USP10 with p62 promoted protein aggregation and aggresome formation (Figure 5). Analysis using USP10 deletion mutants showed that both N- and C-terminal regions of USP10 interact with p62 and that these two regions are required for maximum aggresome-promoting activity (Figure 2F). These results suggested that multiple interactions between USP10 and p62 are required for

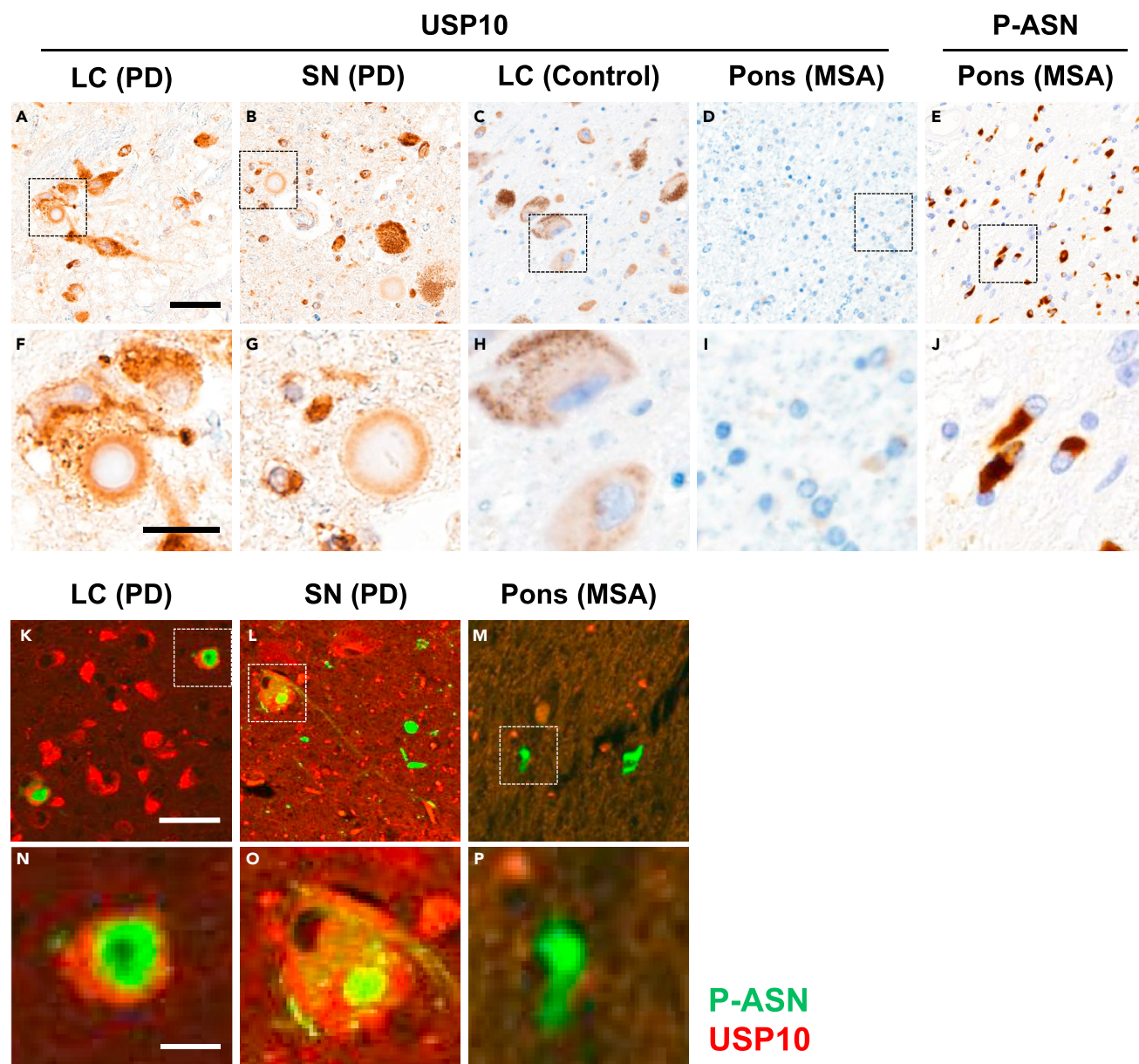


Figure 7. Localizations of USP10 and α -Synuclein in Brain

(A–J) Representative images taken from USP10- or phosphorylated α -synuclein (P-ASN)-immunostained sections of patients with PD (PD, $n = 3$), patients with MSA (MSA, $n = 3$), and controls ($n = 3$). (A–D) and (F–I) USP10 staining; (E and J) P-ASN staining. (F–J) The magnified images of (A–E). (A and F) Locus coeruleus (LC) of PD; (B and G) substantia nigra (SN) of PD; (C and H) LC of control; (D, E, I, and J) pons of MSA.

(K–P) Images of double-immunofluorescence staining of USP10 and P-ASN. (N–P): magnified images of (K–M). (K and N) LC of PD; (L and O) SN of PD; (M and P) pons of MSA. Scale bars, 50 μm in (A–E and K–M) and 10 μm in (F–J and N–P).

See also [Table S1](#).

maximum aggresome-promoting activity of USP10. It should be noted that p62-KD reduced protein aggregation and aggresome formation induced by USP10/CFTR- Δ F508, and the reduction was approximately half of the p62-competent cells (Figures 5A and 5B). Since several ubiquitin receptors other than p62, such as optineurin, neighbor of BRCA1 gene 1 (NBR1), and autophagy-linked FYVE (ALFY) (Rogov et al., 2014), are involved in autophagy, we cannot exclude the possibility that USP10 promotes protein aggregation and aggresome formation by interacting with other ubiquitin receptors in addition to p62.

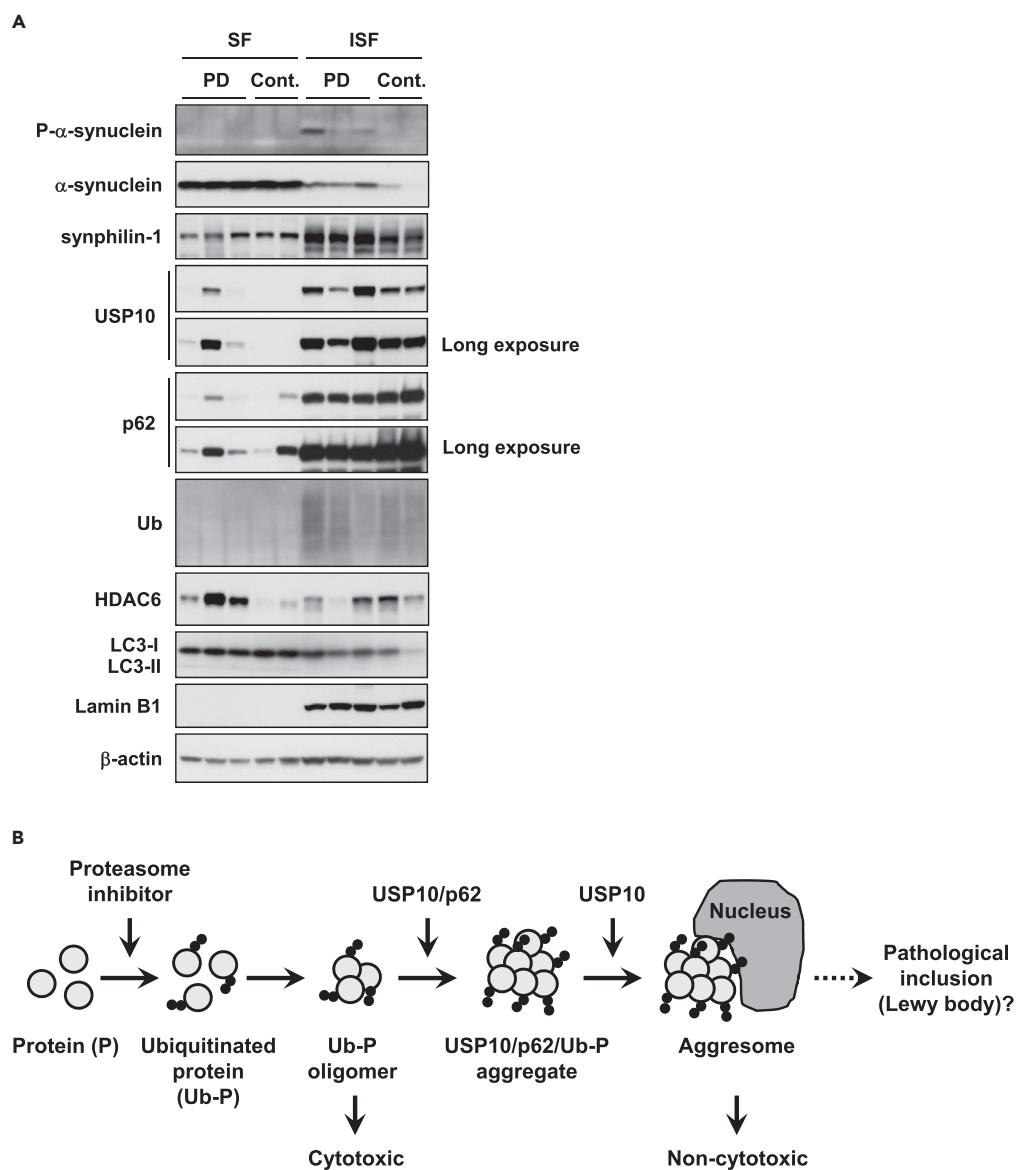


Figure 8. Expression Levels of USP10 and Aggresome-Related Proteins in Brain Lesions of Patients with PD

(A) Triton X-100-soluble fractions (SF) and Triton X-100-insoluble fractions (ISF) were prepared from brain tissues (amygdala) of three patients with PD (PD) and two controls (Cont.), and the lysates were characterized by western blot using anti-phosphorylated α -synuclein, anti- α -synuclein, anti-synphilin-1, anti-USP10, anti-p62, anti-Ub, anti-HDAC6, anti-LC3, anti-Lamin B1, and anti- β -actin antibodies. See also [Table S2](#).

(B) A current model describing the function of USP10 on protein aggregation.

USP10 inhibited cell death induced by PI, and the inhibition correlated with aggresome/aggregate-inducing activity (Figures 6 and S5). Accumulating evidence shows that protein oligomers, but not large protein aggregates, have potent cytotoxic activity (Ramdzan et al., 2017). Thus, USP10-induced aggregates/aggresomes might inhibit apoptosis by reducing the amount of ubiquitinated protein oligomers. This mechanism was supported by the following two findings. Although p62 promotes ubiquitinated protein aggregation, large p62 aggregates detected even in USP10-KD cells inhibited apoptosis as efficiently as aggresomes (Figure 6C). Like USP10-KD, p62-KD increased apoptosis induced by treatment with PI (Figures 6E and 6F). However, we could not exclude the possibility that USP10 inhibits apoptosis by promoting degradation of pro-apoptotic protein(s) by aggresome-mediated autophagy.

PI treatment in USP10-WT cells induced p62/HDAC6-double-positive aggresomes, whereas in USP10-KD cells, it induced many small p62-positive/HDAC6-negative aggregates throughout the cytoplasm (Figures 1C and 1D). These results suggested that USP10 functions to stimulate transport of p62 aggregates to the perinuclear aggresome formation site. HDAC6 promotes aggresome formation by stimulating the transport of p62 aggregates to the perinuclear region (Kawaguchi et al., 2003; Yan et al., 2013). Collectively, these results suggest that USP10 stimulates HDAC6-mediated aggresome-inducing activity. Further analysis is required to understand fully how USP10 promotes aggresome formation.

Formation of inclusions containing ubiquitinated proteins is pathognomonic in various neurodegenerative disorders, including PD and Alzheimer disease (Dantuma and Bott, 2014). Accumulating evidence suggests that aggresome-related mechanisms are involved in the formation of the inclusions, including Lewy bodies (Olanow et al., 2004). The findings herein are consistent with this notion. USP10 was detected in the peripheral portion (halo) of Lewy bodies in patients with PD (Figures 7A, 7B, 7F, and 7G). In addition, the amounts of soluble and insoluble USP10 proteins in brain lesions (amygdala) of patients with PD were more than those of the controls (Figure 8A). In cultured cells, USP10 promoted α -synuclein-induced aggresome formation (Figure 3A) and USP10 was often detected at the periphery of α -synuclein-positive aggresomes (Figures S3C and 3C). These results suggest that USP10 may be a factor associated with the formation of Lewy bodies through an aggresome-related mechanism. In contrast, USP10 was not detected in the α -synuclein-positive GCIs in patients with MSA (Figures 7D and 7I), although the GCIs are immunoreactive for several aggresome-marker proteins, including HDAC6 and p62 (Chiba et al., 2012). Thus, the USP10-dependent aggresome-related mechanism is involved in the formation of Lewy bodies, but not GCIs. This difference might be associated with the different physiological expression level of USP10 between neurons and oligodendrocytes.

Based on the data presented above, we propose the following model for USP10 activity in aggresome and pathogenic inclusion formation (Figure 8B). Ubiquitinated proteins generated by various stresses, especially their oligomers, are highly cytotoxic. These ubiquitinated proteins bind to p62 and USP10, and the formed aggregates inhibit proteasome activity to further increase the amount of ubiquitinated proteins. These ubiquitinated proteins then form aggresomes. Thus, USP10 and p62 promote cell survival by reducing the amount of cytotoxic ubiquitinated protein monomers and oligomers. In addition, ubiquitinated proteins in aggresomes are degraded by autophagy or proteasome-mediated degradation, which reduces the amount of ubiquitinated proteins. However, continuous dysfunction of proteasomes and/or autophagy produces pathogenic inclusions such as Lewy bodies. Collectively, we propose that USP10 is an attractive target to control aberrant aggregation and/or cytotoxicity of ubiquitinated proteins in protein aggregation-related diseases including PD.

Limitations of the Study

We showed that USP10 promotes protein aggregation and aggresome formation by inhibiting the proteasome-mediated degradation of ubiquitinated proteins. It should be noted that ubiquitinated proteins are also degraded by autophagy. In addition, some ubiquitinated proteins such as α -synuclein are secreted from cells. Thus, USP10 might have another activity to promote protein aggregations. Further analysis is required to elucidate how USP10 promotes protein aggregation and aggresome formation.

We proposed that GCI is generated by a USP10-independent mechanism within oligodendrocytes. α -synuclein inclusions have been shown to propagate cell-to-cell by a prion-like mechanism. Thus, GCI might be formed in oligodendrocytes by the endocytosis of extracellular α -synuclein inclusions secreted from other cells such as neurons. Further analysis is required to elucidate how USP10-negative GCI is formed in oligodendrocytes.

METHODS

All methods can be found in the accompanying [Transparent Methods supplemental file](#).

SUPPLEMENTAL INFORMATION

Supplemental Information includes Transparent Methods, five figures, and two tables and can be found with this article online at <https://doi.org/10.1016/j.isci.2018.11.006>.

ACKNOWLEDGMENTS

We thank Dr. Hiroyuki Miyoshi (Keio University) and the RIKEN BioResource Center (Tsukuba, Japan) for the lentiviral packaging plasmids; Dr. Ron Kopito (Stanford University, California) for the GFP-CFTR-ΔF508 plasmid; Dr. Masato Hasegawa (Tokyo Metropolitan Institute of Medical Science, Japan) for the α -synuclein plasmid; Dr. Kah-Leong Lim (National Neuroscience Institute, Singapore) for the GFP- α -synuclein, Myc-synphilin-1, and HA-AIMP2 plasmids; and Dr. Dirk Bohmann (University of Rochester Medical Center, NY) for the His-ubiquitin plasmid. We also thank Misako Tobimatsu for technical assistance. This work was supported in part by JSPS KAKENHI grant numbers 26670222, 15H04704, 16K15502, 26461417, and 17K09918; research grants from the Takeda Science Foundation; the Strategic Research Program for Brain Sciences from Japan AMED; and the Collaborative Research Project of the Brain Research Institute, Niigata University. We thank the Edanz Group (www.edanzediting.com/ac) for editing a draft of this manuscript.

AUTHOR CONTRIBUTIONS

M.T. performed most of the experiments and data analysis and wrote the manuscript. H.K., A.K. and L.Z. performed pathological analysis using brain tissues. Y.I. prepared rat primary-neuron-enriched cells. T.K., Y.K., M.N., H.N., M.H., and M.K. provided critical suggestions throughout the manuscript. M.F. designed and supervised the study and wrote the manuscript.

DECLARATION OF INTERESTS

The authors declare no competing interests.

Received: April 23, 2018

Revised: September 19, 2018

Accepted: November 1, 2018

Published: November 30, 2018

REFERENCES

- Ahmed, Z., Asi, Y.T., Sailer, A., Lees, A.J., Houlden, H., Revesz, T., and Holton, J.L. (2012). The neuropathology, pathophysiology and genetics of multiple system atrophy. *Neuropathol. Appl. Neurobiol.* *38*, 4–24.
- Anderson, J.P., Walker, D.E., Goldstein, J.M., de Laat, R., Banducci, K., Caccavello, R.J., Barbour, R., Huang, J., Kling, K., Lee, M., et al. (2006). Phosphorylation of Ser-129 is the dominant pathological modification of alpha-synuclein in familial and sporadic Lewy body disease. *J. Biol. Chem.* *281*, 29739–29752.
- Calderilla-Barbosa, L., Seibenhener, M.L., Du, Y., Diaz-Meco, M.T., Moscat, J., Yan, J., Wooten, M.W., and Wooten, M.C. (2014). Interaction of SQSTM1 with the motor protein dynein–SQSTM1 is required for normal dynein function and trafficking. *J. Cell Sci.* *127*, 4052–4063.
- Cheng, S.H., Gregory, R.J., Marshall, J., Paul, S., Souza, D.W., White, G.A., O’Riordan, C.R., and Smith, A.E. (1990). Defective intracellular transport and processing of CFTR is the molecular basis of most cystic fibrosis. *Cell* *63*, 827–834.
- Chiba, Y., Takei, S., Kawamura, N., Kawaguchi, Y., Sasaki, K., Hasegawa-Ishii, S., Furukawa, A., Hosokawa, M., and Shimada, A. (2012). Immunohistochemical localization of aggresomal proteins in glial cytoplasmic inclusions in multiple system atrophy. *Neuropathol. Appl. Neurobiol.* *38*, 559–571.
- Cohen-Kaplan, V., Livneh, I., Avni, N., Fabre, B., Ziv, T., Kwon, Y.T., and Ciechanover, A. (2016). p62- and ubiquitin-dependent stress-induced autophagy of the mammalian 26S proteasome. *Proc. Natl. Acad. Sci. U S A* *113*, E7490–E7499.
- Corti, O., Hampe, C., Koutnikova, H., Darios, F., Jacquier, S., Prigent, A., Robinson, J.C., Pradier, L., Ruberg, M., Mirande, M., et al. (2003). The p38 subunit of the aminoacyl-tRNA synthetase complex is a Parkin substrate: linking protein biosynthesis and neurodegeneration. *Hum. Mol. Genet.* *12*, 1427–1437.
- Dantuma, N.P., and Bott, L.C. (2014). The ubiquitin-proteasome system in neurodegenerative diseases: precipitating factor, yet part of the solution. *Front. Mol. Neurosci.* *7*, 70.
- Deng, M., Yang, X., Qin, B., Liu, T., Zhang, H., Guo, W., Lee, S.B., Kim, J.J., Yuan, J., Pei, H., et al. (2016). Deubiquitination and activation of AMPK by USP10. *Mol. Cell* *61*, 614–624.
- Engelender, S., Kaminsky, Z., Guo, X., Sharp, A.H., Amaravi, R.K., Kleiderlein, J.J., Margolis, R.L., Troncoso, J.C., Lanahan, A.A., Worley, P.F., et al. (1999). Synphilin-1 associates with alpha-synuclein and promotes the formation of cytosolic inclusions. *Nat. Genet.* *22*, 110–114.
- Garcia-Mata, R., Bebok, Z., Sorscher, E.J., and Sztul, E.S. (1999). Characterization and dynamics of aggresome formation by a cytosolic GFP-chimera. *J. Cell Biol.* *146*, 1239–1254.
- Gilon, T., Chomsky, O., and Kulka, R.G. (1998). Degradation signals for ubiquitin system proteolysis in *Saccharomyces cerevisiae*. *EMBO J.* *17*, 2759–2766.
- Higuchi, M., Kawamura, H., Matsuki, H., Hara, T., Takahashi, M., Saito, S., Saito, K., Jiang, S., Naito, M., Kiyonari, H., and Fujii, M. (2016). USP10 is an essential deubiquitinase for hematopoiesis and inhibits apoptosis of long-term hematopoietic stem cells. *Stem Cell Reports* *7*, 1116–1129.
- Hipp, M.S., Park, S.H., and Hartl, F.U. (2014). Proteostasis impairment in protein-misfolding and -aggregation diseases. *Trends Cell Biol.* *24*, 506–514.
- Ichimura, Y., Waguri, S., Sou, Y.S., Kageyama, S., Hasegawa, J., Ishimura, R., Saito, T., Yang, Y., Kouno, T., Fukutomi, T., et al. (2013). Phosphorylation of p62 activates the Keap1-Nrf2 pathway during selective autophagy. *Mol. Cell* *51*, 618–631.
- Jain, A., Lamark, T., Sjøttem, E., Larsen, K.B., Awuh, J.A., Overvatn, A., McMahon, M., Hayes, J.D., and Johansen, T. (2010). p62/SQSTM1 is a target gene for transcription factor NRF2 and creates a positive feedback loop by inducing antioxidant response element-driven gene transcription. *J. Biol. Chem.* *285*, 22576–22591.
- Jaramillo, M.C., and Zhang, D.D. (2013). The emerging role of the Nrf2-Keap1 signaling pathway in cancer. *Genes Dev.* *27*, 2179–2191.
- Johansen, T., and Lamark, T. (2014). Selective autophagy mediated by autophagic adapter proteins. *Autophagy* *7*, 279–296.
- Johnston, J.A., Ward, C.L., and Kopito, R.R. (1998). Aggresomes: a cellular response to misfolded proteins. *J. Cell Biol.* *143*, 1883–1898.

- Katsuragi, Y., Ichimura, Y., and Komatsu, M. (2015). p62/SQSTM1 functions as a signaling hub and an autophagy adaptor. *FEBS J.* **282**, 4672–4678.
- Kawaguchi, Y., Kovacs, J.J., McLaurin, A., Vance, J.M., Ito, A., and Yao, T.P. (2003). The deacetylase HDAC6 regulates aggresome formation and cell viability in response to misfolded protein stress. *Cell* **115**, 727–738.
- Ko, H.S., von Coelln, R., Sriram, S.R., Kim, S.W., Chung, K.K., Pletnikova, O., Troncoso, J., Johnson, B., Saffary, R., Goh, E.L., et al. (2005). Accumulation of the authentic parkin substrate aminoacyl-tRNA synthetase cofactor, p38/JTV-1, leads to catecholaminergic cell death. *J. Neurosci.* **25**, 7968–7978.
- Komatsu, M., Waguri, S., Koike, M., Sou, Y.S., Ueno, T., Hara, T., Mizushima, N., Iwata, J., Ezaki, J., Murata, S., et al. (2007). Homeostatic levels of p62 control cytoplasmic inclusion body formation in autophagy-deficient mice. *Cell* **131**, 1149–1163.
- Kopito, R.R. (2000). Aggresomes, inclusion bodies and protein aggregation. *Trends Cell Biol.* **10**, 524–530.
- Lamark, T., and Johansen, T. (2010). Autophagy: links with the proteasome. *Curr. Opin. Cell Biol.* **22**, 192–198.
- Lin, Z., Yang, H., Tan, C., Li, J., Liu, Z., Quan, Q., Kong, S., Ye, J., Gao, B., and Fang, D. (2013). USP10 antagonizes c-Myc transcriptional activation through SIRT6 stabilization to suppress tumor formation. *Cell Rep.* **5**, 1639–1649.
- Luciani, A., Vilella, V.R., Esposito, S., Brunetti-Pierri, N., Medina, D., Settembre, C., Gavina, M., Pulze, L., Giardino, I., Pettoello-Mantovani, M., et al. (2010). Defective CFTR induces aggresome formation and lung inflammation in cystic fibrosis through ROS-mediated autophagy inhibition. *Nat. Cell Biol.* **12**, 863–875.
- Lukacs, G.L., and Verkman, A.S. (2012). CFTR: folding, misfolding and correcting the DeltaF508 conformational defect. *Trends Mol. Med.* **18**, 81–91.
- Menendez-Benito, V., Verhoef, L.G., Masucci, M.G., and Dantuma, N.P. (2005). Endoplasmic reticulum stress compromises the ubiquitin-proteasome system. *Hum. Mol. Genet.* **14**, 2787–2799.
- Olanow, C.W., Perl, D.P., DeMartino, G.N., and McNaught, K.S.P. (2004). Lewy-body formation is an aggresome-related process: a hypothesis. *Lancet Neurol.* **3**, 496–503.
- Pankiv, S., Clausen, T.H., Lamark, T., Brech, A., Bruun, J.A., Outzen, H., Overvatn, A., Bjorkoy, G., and Johansen, T. (2007). p62/SQSTM1 binds directly to Atg8/LC3 to facilitate degradation of ubiquitinated protein aggregates by autophagy. *J. Biol. Chem.* **282**, 24131–24145.
- Peng, C., Gathagan, R.J., and Lee, V.M. (2017). Distinct alpha-Synuclein strains and implications for heterogeneity among alpha-Synucleinopathies. *Neurobiol. Dis.* **109** (Pt B), 209–218.
- Ramdzan, Y.M., Trubetskov, M.M., Ormsby, A.R., Newcombe, E.A., Sui, X., Tobin, M.J., Bongiovanni, M.N., Gras, S.L., Dewson, G., Miller, J.M.L., et al. (2017). Huntingtin inclusions trigger cellular quiescence, deactivate apoptosis, and lead to delayed necrosis. *Cell Rep.* **19**, 919–927.
- Rogov, V., Dotsch, V., Johansen, T., and Kirkin, V. (2014). Interactions between autophagy receptors and ubiquitin-like proteins form the molecular basis for selective autophagy. *Mol. Cell* **53**, 167–178.
- Ross, C.A., and Poirier, M.A. (2004). Protein aggregation and neurodegenerative disease. *Nat. Med.* **10** Suppl, S10–S17.
- Shen, D., Coleman, J., Chan, E., Nicholson, T.P., Dai, L., Sheppard, P.W., and Patton, W.F. (2011). Novel cell- and tissue-based assays for detecting misfolded and aggregated protein accumulation within aggresomes and inclusion bodies. *Cell Biochem. Biophys.* **60**, 173–185.
- Spillantini, M.G., Schmidt, M.L., Lee, V.M., Trojanowski, J.Q., Jakes, R., and Goedert, M. (1997). Alpha-synuclein in Lewy bodies. *Nature* **388**, 839–840.
- Takahashi, M., Higuchi, M., Makokha, G.N., Matsuki, H., Yoshita, M., Tanaka, Y., and Fujii, M. (2013a). HTLV-1 Tax oncoprotein stimulates ROS production and apoptosis in T cells by interacting with USP10. *Blood* **122**, 715–725.
- Takahashi, M., Higuchi, M., Matsuki, H., Yoshita, M., Ohsawa, T., Oie, M., and Fujii, M. (2013b). Stress granules inhibit apoptosis by reducing reactive oxygen species production. *Mol. Cell Biol.* **33**, 815–829.
- Tanaka, M., Kim, Y.M., Lee, G., Junn, E., Iwatsubo, T., and Mouradian, M.M. (2004). Aggresomes formed by alpha-synuclein and synphilin-1 are cytoprotective. *J. Biol. Chem.* **279**, 4625–4631.
- Tomko, R.J., Jr., and Hochstrasser, M. (2013). Molecular architecture and assembly of the eukaryotic proteasome. *Annu. Rev. Biochem.* **82**, 415–445.
- Yan, J., Seibenhener, M.L., Calderilla-Barbosa, L., Diaz-Meco, M.T., Moscat, J., Jiang, J., Wooten, M.W., and Wooten, M.C. (2013). SQSTM1/p62 interacts with HDAC6 and regulates deacetylase activity. *PLoS One* **8**, e76016.
- Yuan, J., Luo, K., Zhang, L., Cheville, J.C., and Lou, Z. (2010). USP10 regulates p53 localization and stability by deubiquitinating p53. *Cell* **140**, 384–396.

ISCI, Volume 9

Supplemental Information

USP10 Is a Driver of Ubiquitinated Protein Aggregation and Aggresome Formation to Inhibit Apoptosis

Masahiko Takahashi, Hiroki Kitaura, Akiyoshi Kakita, Taichi Kakihana, Yoshinori Katsuragi, Masaaki Nameta, Lu Zhang, Yuriko Iwakura, Hiroyuki Nawa, Masaya Higuchi, Masaaki Komatsu, and Masahiro Fujii

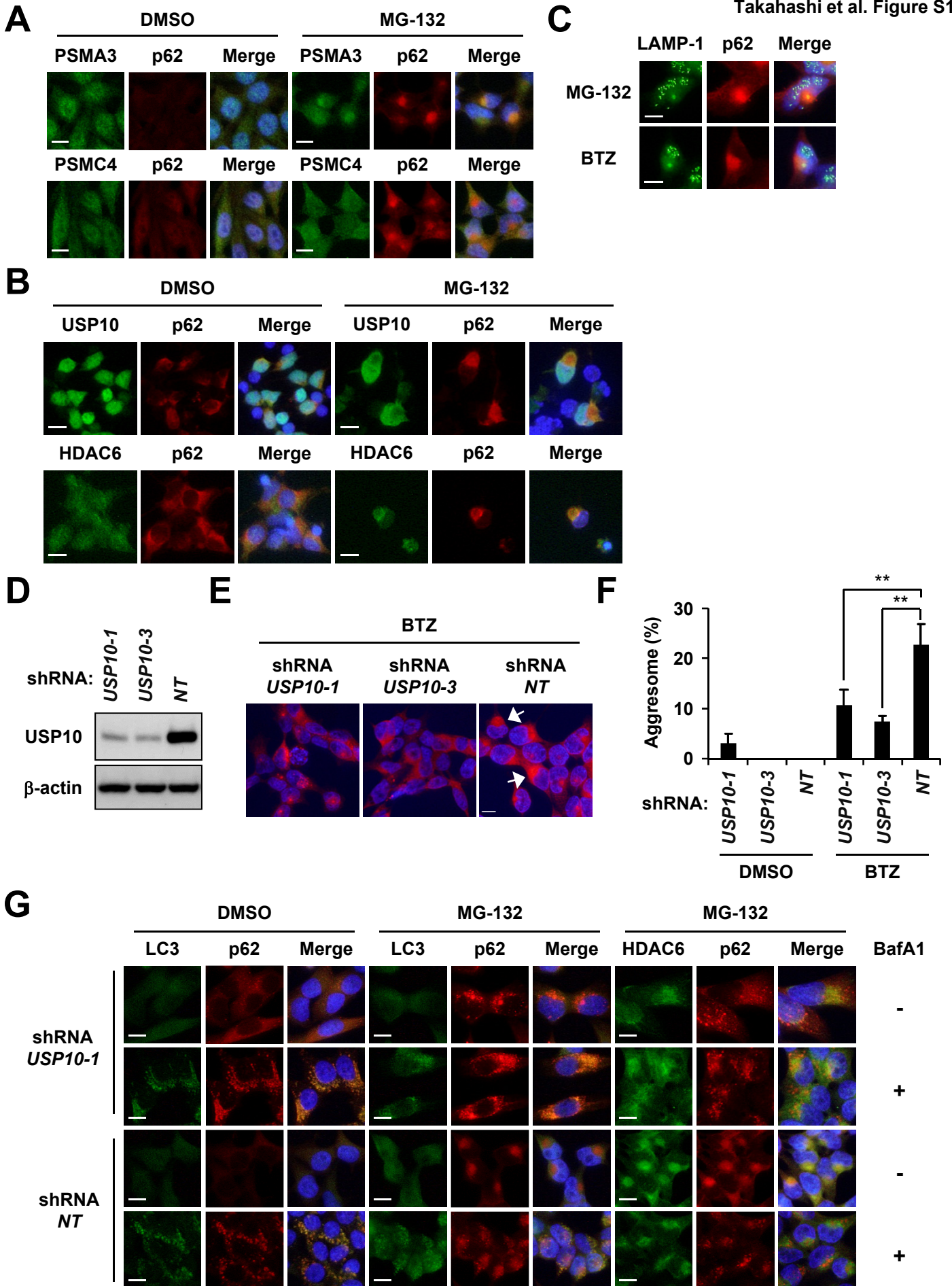


Figure S1, related to Figure 1. USP10 promotes the transport of p62 aggregates to the perinuclear region for aggresome formation

(A) HeLa cells were treated with 5 μ M MG-132 or DMSO for 12 hr, and the cells were stained with the anti-p62 (red) antibody and with either the anti-PSMA3 (green) or anti-PSMC4 (green) antibody. Nuclei were counterstained using Hoechst33258 (blue). The bars indicate 10 μ m.

(B) Primary neuron-enriched cells prepared from cortical tissues of rat embryo were treated with 2 μ M MG-132 or DMSO for 8 hr, and the cells were stained with the anti-p62 (red) antibody together with either the anti-USP10 (green) or anti-HDAC6 (green) antibody. Nuclei were counterstained using Hoechst33258 (blue). The bars indicate 10 μ m.

(C) HeLa cells were treated with MG-132 or 1 μ M bortezomib (BTZ) for 12 hr, and the cells were stained with anti-LAMP1 (green) and anti-p62 (red) antibodies, and with Hoechst33258 (blue). The bars indicate 10 μ m.

(D) 293T cells were infected with lentivirus encoding *USP10* shRNA (*USP10-1* or *USP10-3*) or control siRNA (*NT*). Whole-cell extracts were characterized using western blot analysis (WB) with anti-USP10 and anti- β -actin antibodies.

(E) USP10-KD (*USP10-1* or *USP10-3*) and control (*NT*) 293T cells were treated with 2 μ M BTZ or DMSO for 9 hr, and the cells were stained with anti-p62 (red) antibody and Hoechst33258 (blue). Arrows indicate aggresomes (more than 15 μ m² in size at the perinuclear region with nuclear deformity). The bar indicates 10 μ m.

(F) The proportions of cells containing aggresome are presented as the mean \pm s.d. ($n = 3$); ** $P < 0.01$.

(G) USP10-KD (*USP10-1*) and control (*NT*) HeLa cells were pretreated with 10 nM BafA1 or DMSO and further treated with MG-132 or DMSO for 12 hr. The cells were stained with anti-LC3 (green) and anti-p62 (red) antibodies, and anti-HDAC6 (green) and anti-p62 (red) antibodies. Nuclei were counterstained using Hoechst33258 (blue). The bars indicate 10 μ m.

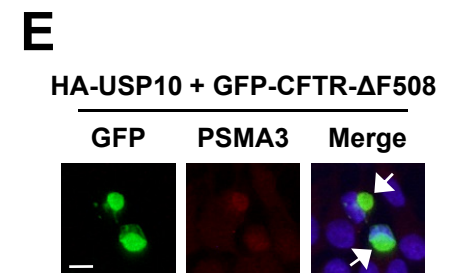
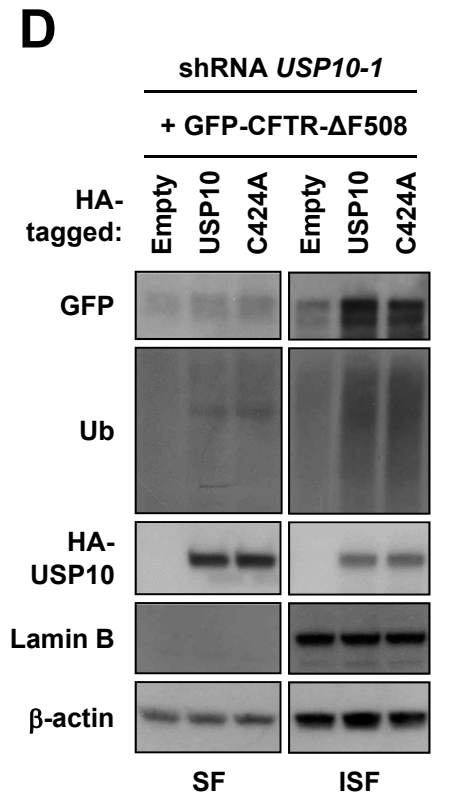
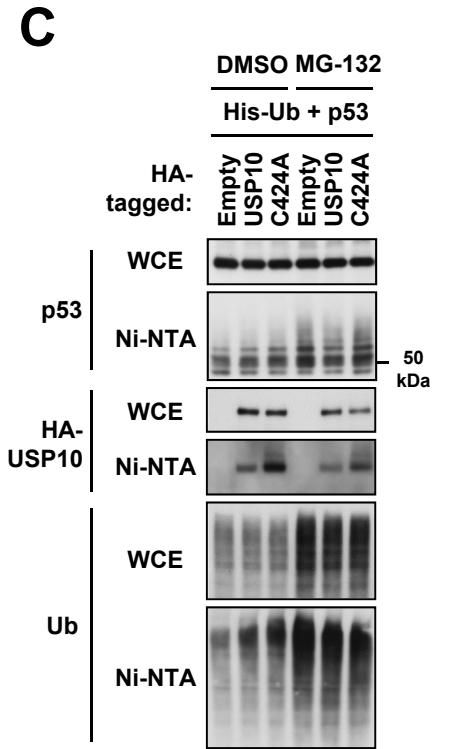
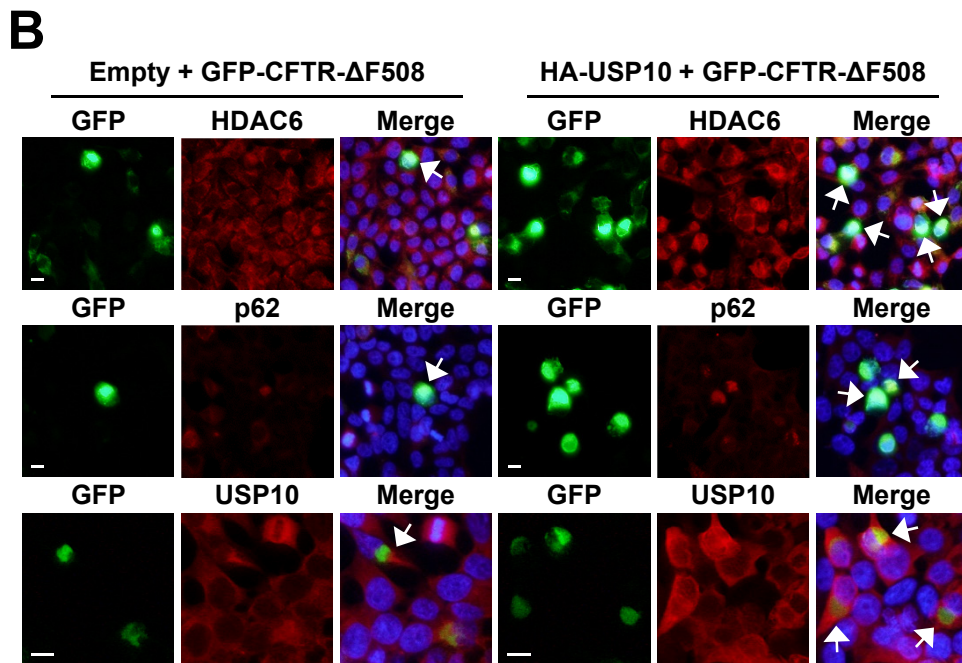
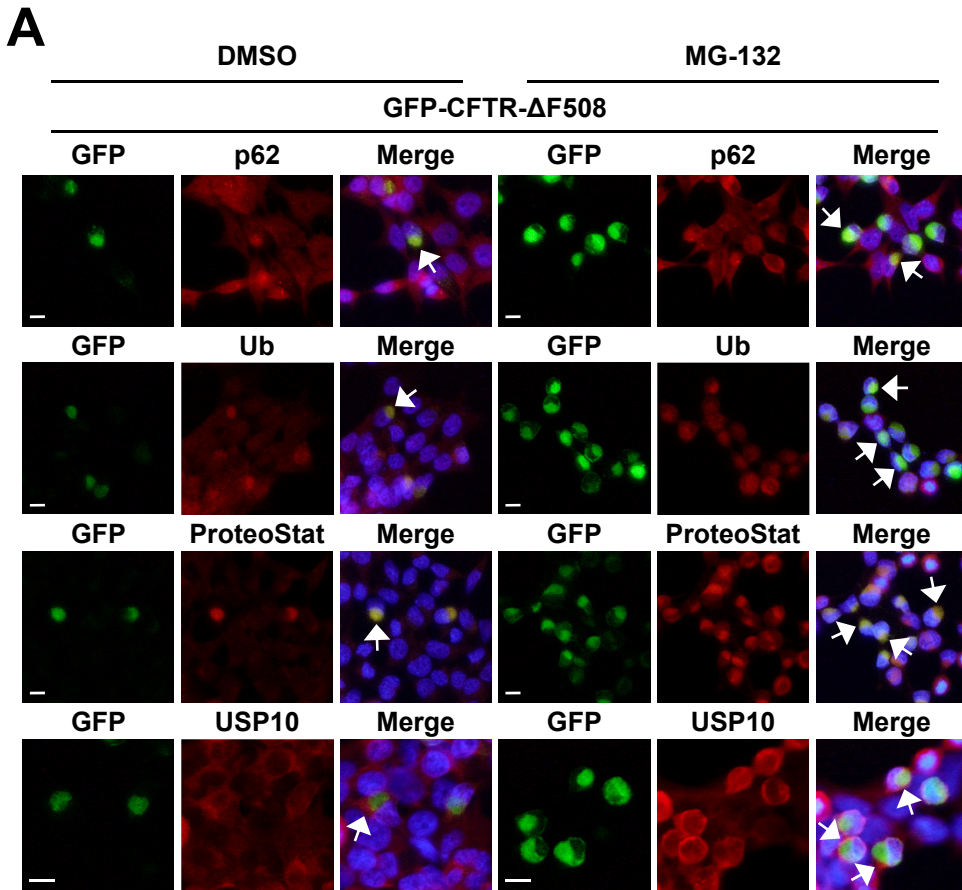


Figure S2, related to Figure 2. CFTR-ΔF508 co-localizes with aggresome markers

(A) HeLa cells were transfected with the GFP-CFTR-ΔF508 plasmid and treated with 5 μM MG-132 or DMSO for 12 hr, and the cells were stained with the anti-p62 antibody (red), anti-ubiquitin (Ub) antibody (red), ProteoStat dye (red) or anti-USP10 (red) antibody and Hoechst33258 (blue). Arrows indicate localization of each aggresome marker at CFTR-ΔF508-induced aggresomes. The bars indicate 10 μm.

(B) HeLa cells were transfected with the HA-USP10 and the GFP-CFTR-ΔF508 plasmids, and these cells were stained with the anti-HDAC6 (red), anti-p62 (red) or USP10 (red) antibody and Hoechst33258 (blue). Arrows indicate localization of each protein at CFTR-ΔF508-induced aggresomes. The bars indicate 10 μm.

(C) HeLa cells were transfected with the His-Ub and p53 plasmids together with HA-USP10 or its deubiquitinase-dead mutant USP10^{C424A} plasmid. Ubiquitinated proteins in cell lysates were collected by Ni-NTA-agarose (Ni-NTA). The whole cell extracts (WCE) and His-ubiquitinated proteins eluted from Ni-NTA agarose were characterized by WB using anti-p53, anti-HA and anti-Ub antibodies.

(D) USP10-KD (*USP10-1*) HeLa cells were transfected with HA-USP10 or its deubiquitinase-dead mutant USP10^{C424A} plasmid together with the GFP-CFTR-ΔF508 plasmid, and NP-40-soluble fractions (SF) and NP40-insoluble fractions (ISF) were characterized by WB using anti-GFP, anti-Ub, anti-HA, anti-Lamin B and anti-β-actin antibodies.

(E) HeLa cells were transfected with the HA-USP10 and GFP-CFTR-ΔF508 plasmids, and these cells were stained with the anti-PSMA3 (red) antibody and Hoechst33258 (blue). Arrows indicate localization of PSMA3 at CFTR-ΔF508-induced aggresomes. The bar indicates 10 μm.

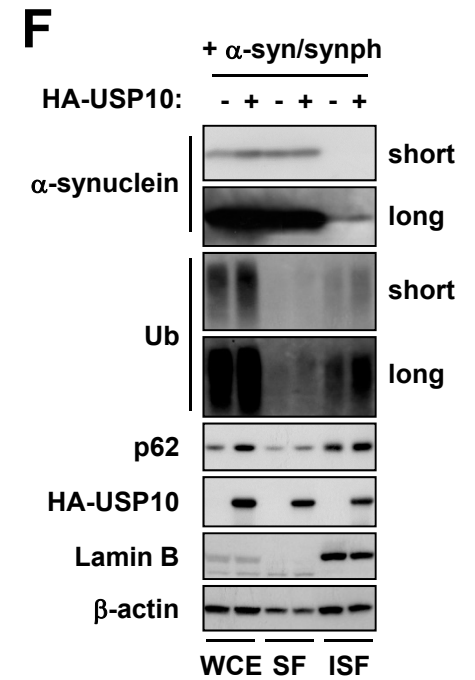
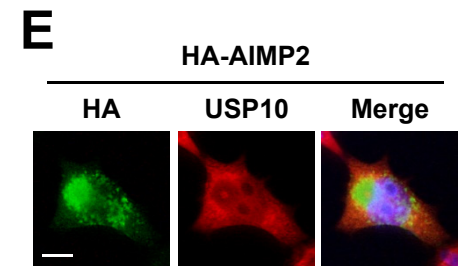
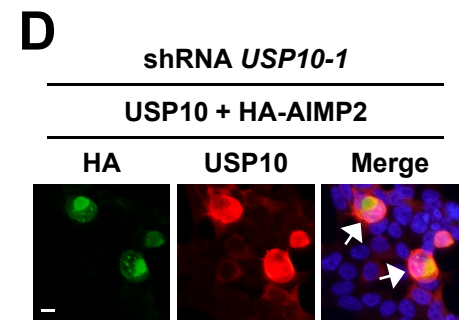
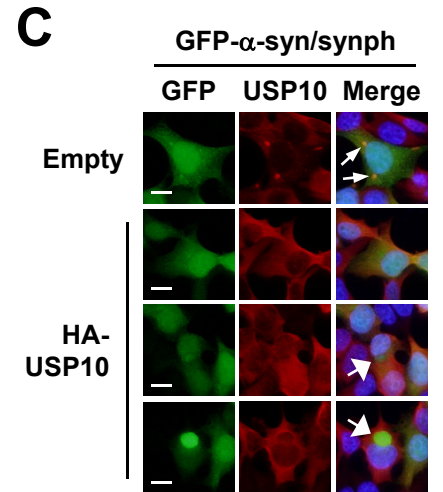
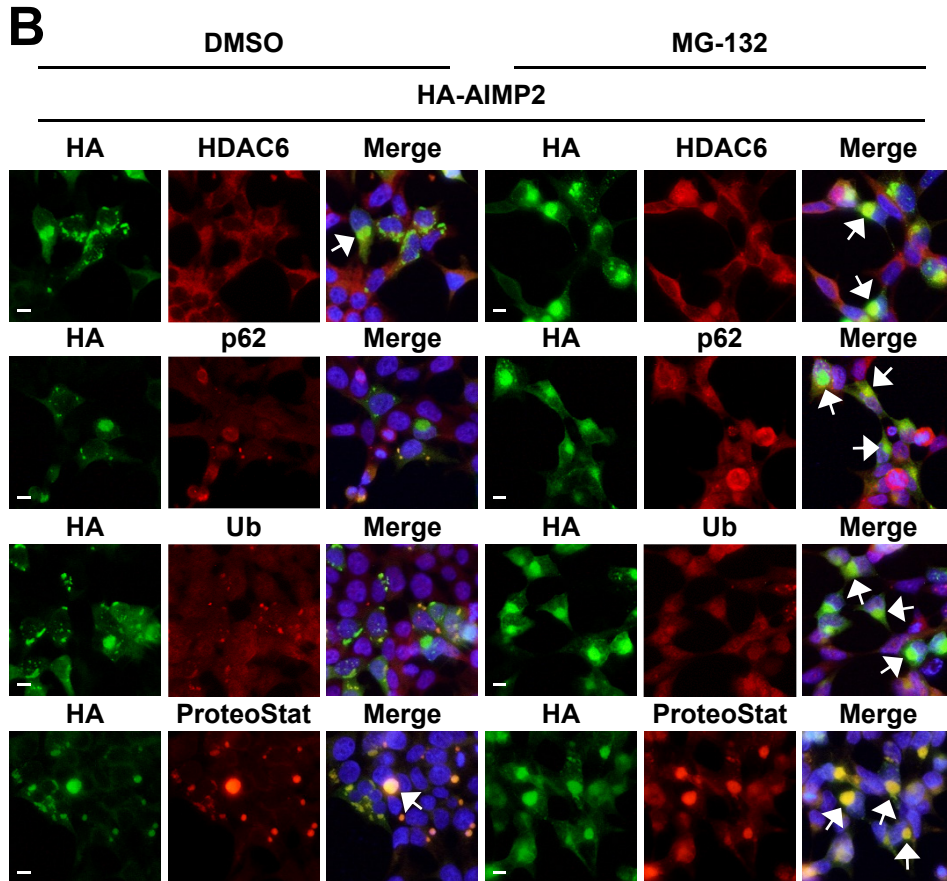
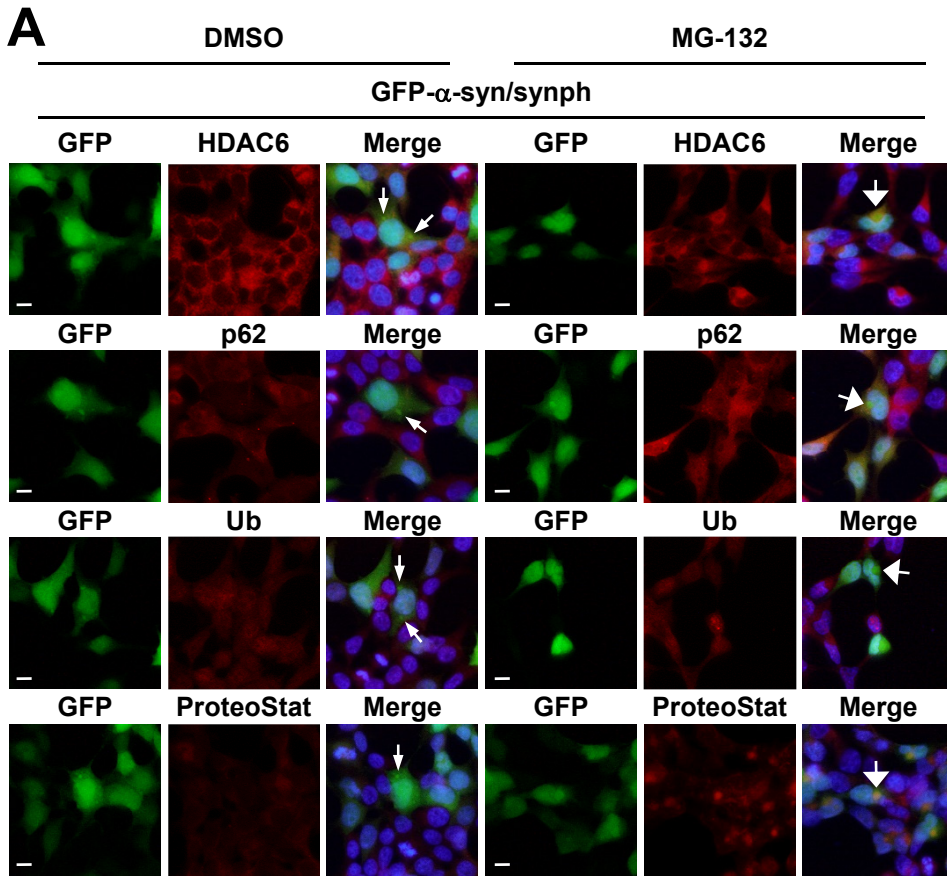


Figure S3, related to Figure 3. α -Synuclein or AIMP2 co-localizes with aggresome markers

(A) HeLa cells were transfected with GFP- α -synuclein (GFP- α -syn) and Myc-synphilin-1 (synph) plasmids and treated with 5 μ M MG-132 or DMSO for 12 hr. The cells were stained with the anti-HDAC6 (red), anti-p62 (red) or anti-Ub (red) antibody, or stained with ProteoStat dye (red). Nuclei were counterstained using Hoechst33258 (blue). Small and large arrows indicate α -synuclein-positive aggregates detected under DMSO treatment and α -synuclein-positive aggresome-like aggregates induced by MG-132, respectively. The bars indicate 10 μ m.

(B) HeLa cells were transfected with the HA-AIMP2 plasmid and treated with MG-132 or DMSO for 12 hr. The cells were stained with the anti-HA (green) antibody and with either the anti-HDAC6 (red), anti-p62 (red) or anti-Ub (red) antibody, or stained with ProteoStat dye (red). Nuclei were counterstained using Hoechst33258 (blue). Arrows indicate localization of each aggresome marker at HA-AIMP2-induced aggresomes. The bars indicate 10 μ m.

(C) HeLa cells were transfected with the HA-USP10 and GFP- α -syn/synph plasmids, and the cells were stained with the anti-USP10 (red) antibody and Hoechst33258 (blue). Small arrows indicate α -synuclein-positive aggregates positive for endogenous USP10, whereas the large arrows indicate α -synuclein-positive aggresomes induced by exogenous HA-USP10 expression. The bars indicate 10 μ m.

(D) USP10-KD (*USP10-1*) HeLa cells were transfected with the non-tagged USP10 and the HA-AIMP2 plasmids, and these cells were stained with the anti-HA (green) and anti-USP10 (red) antibodies, and with Hoechst33258 (blue). Arrows indicate HA-AIMP2-positive aggresomes induced by exogenous USP10 expression. The bar indicates 10 μ m.

(E) HeLa cells were transfected with the HA-AIMP2 plasmid, and these cells were stained with the anti-HA (green) and anti-USP10 (red) antibodies, and with Hoechst33258 (blue). The bar indicates 10 μ m.

(F) HeLa cells were transfected with the HA-USP10, α -synuclein (α -syn) and Myc-synphilin-1 (synph) plasmids, and whole-cell extracts (WCE), NP-40-soluble fractions (SF) and NP-40-insoluble fractions (ISF) were characterized by western blot analysis using anti- α -synuclein, anti-Ub, anti-p62, anti-HA, anti-Lamin B and anti- β -actin antibodies.

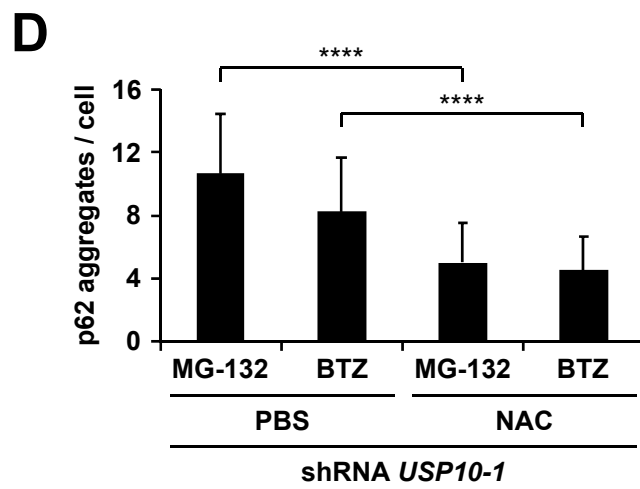
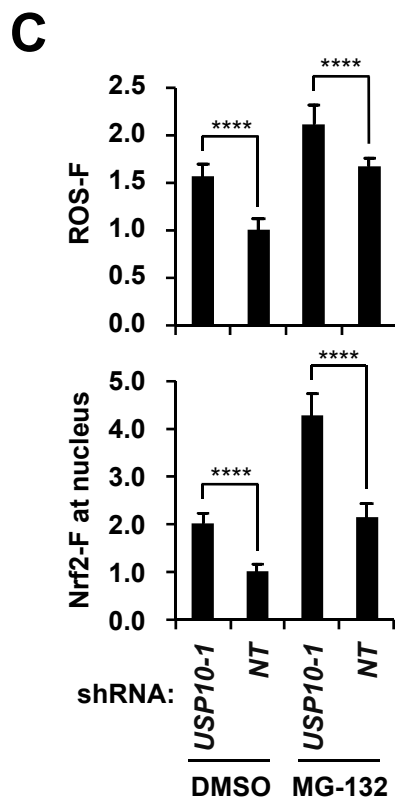
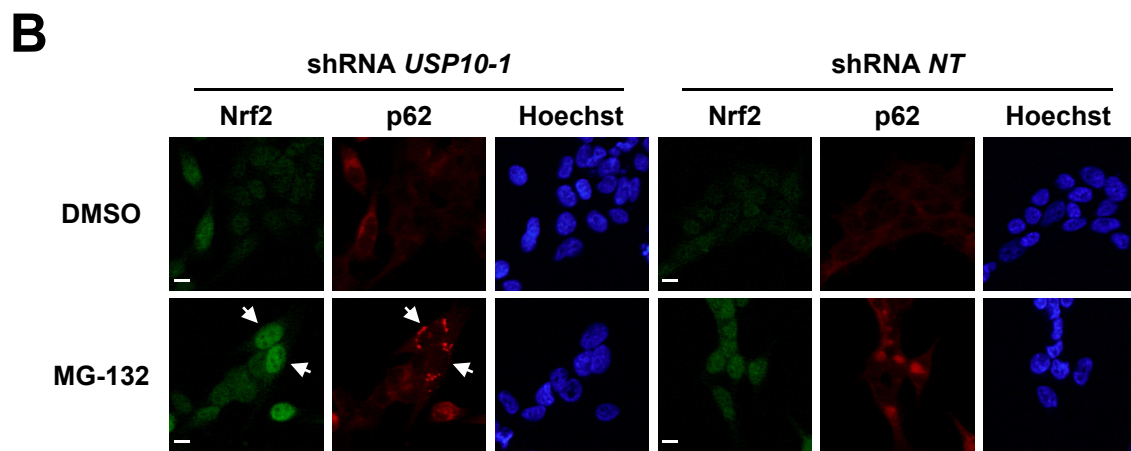
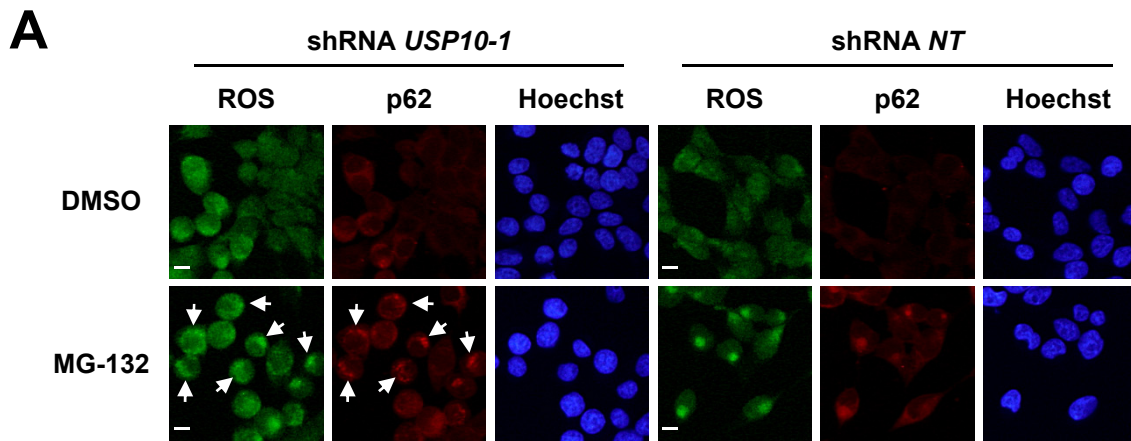


Figure S4, related to Figure 5. ROS accumulation in USP10-knockdown cells activates p62 aggregation

(A) USP10-KD (*USP10-1*) and control (*NT*) HeLa cells were treated with 5 μ M MG-132 or DMSO for 12 hr, and the cells were stained with 5 μ M CM-H₂DCFDA (green) and the anti-p62 (red) antibody, and with Hoechst33258 (blue). Arrows indicate cells with a high amount of ROS and p62 aggregates. The bars indicate 10 μ m.

(B) The indicated HeLa cells were treated with MG-132 or DMSO for 12 hr, and the cells were stained with the anti-Nrf2 (green) and anti-p62 (red) antibodies, and with Hoechst33258 (blue). Arrows indicate cells with a high amount of Nrf2 in the nucleus and p62 aggregates. The bars indicate 10 μ m.

(C) CM-H₂DCFDA fluorescence (ROS-F) or Nrf2 fluorescence at the nucleus (Nrf2-F at nucleus) from panel (A) or (B) are presented as the mean \pm s.d. ($n = 20$); **** $P < 0.0001$.

(D) USP10-KD (*USP10-1*) HeLa cells were pretreated with 20 mM N-acetylcysteine (NAC) or PBS and further treated with MG-132 or 1 μ M bortezomib (BTZ) for 12 hr. The cells were stained with the anti-p62 antibody and the numbers of p62 aggregates per cell were counted. The values denote the mean \pm s.d. ($n = 30$); **** $P < 0.0001$.

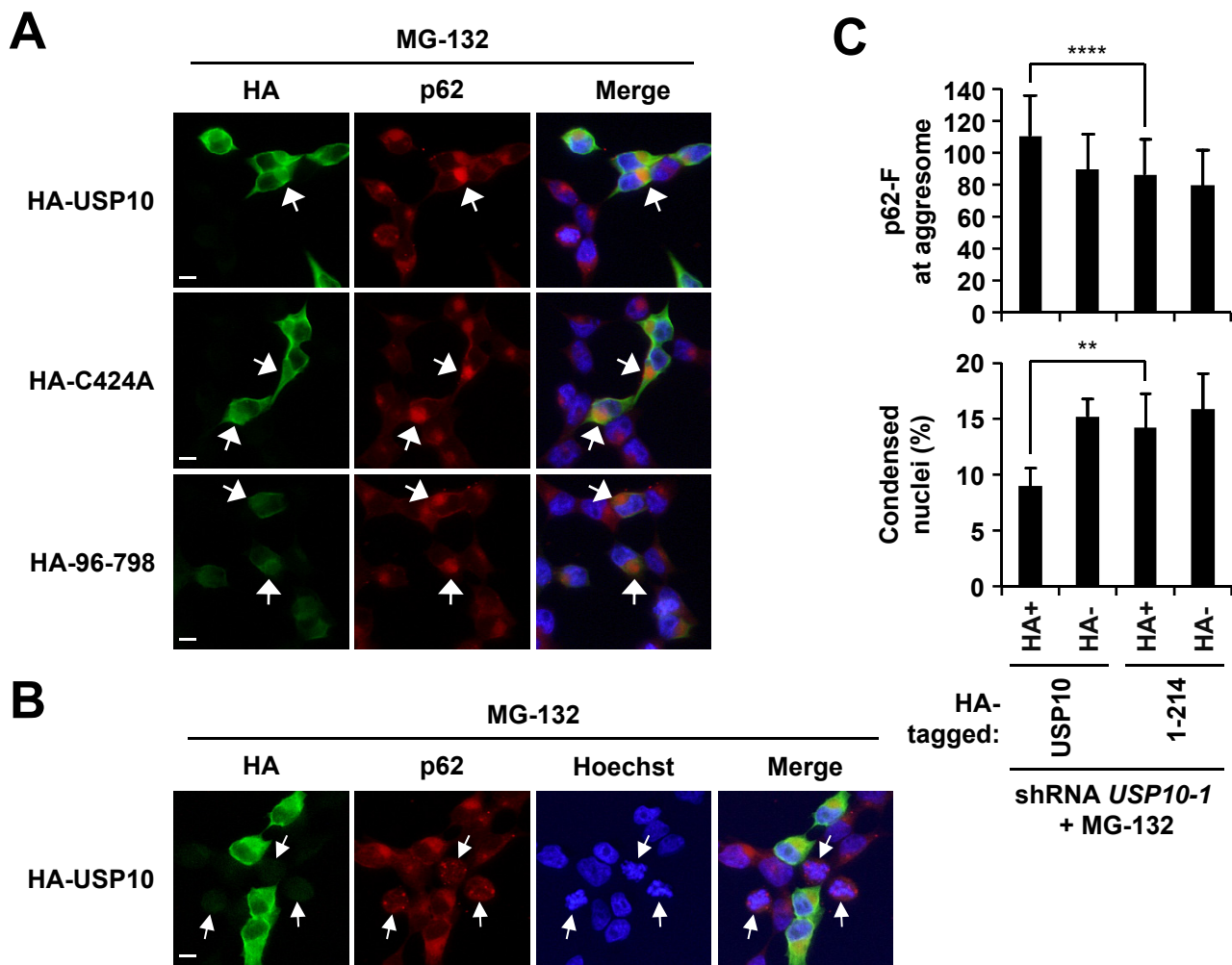


Figure S5, related to Figure 6. Deubiquitinase activity of USP10 is dispensable to inhibit cell death induced by a proteasome inhibitor

(A) USP10-KD (*USP10-1*) HeLa cells were transfected with HA-USP10 or its mutant (USP10^{C424A} or USP10⁹⁶⁻⁷⁹⁸) plasmid, and further treated with 5 μ M MG-132 for 12 hr. Cells were stained with anti-HA (green) and anti-p62 (red) antibodies, and with Hoechst33258 (blue). The arrows indicate cells showing bright p62-fluorescence because of the overexpression of wild-type USP10, USP10^{C424A} or USP10⁹⁶⁻⁷⁹⁸. The bars indicate 10 μ m.

(B) Representative image of cell death (condensed nuclei; blue) without the overexpression of exogenous HA-USP10 (green) after MG-132 treatment is shown by the arrows. The bar indicates 10 μ m.

(C) USP10-KD (*USP10-1*) HeLa cells were transfected with HA-USP10 or its mutant USP10¹⁻²¹⁴ plasmid and further treated with MG-132 for 12 hr. Cells were analysed in a similar manner to (Figure 6G). The values denote the mean \pm s.d. (p62-F at aggresome; $n = 40$, condensed nuclei (%); $n = 6$); ** $P < 0.01$; **** $P < 0.0001$.

Table S1, related to Figure 7. Clinicopathologic profiles of the patients.

Age at death (yrs)	Sex	Clinical Diagnosis	Pathological Diagnosis
Control			
90	M	Myopathy	Myopathy
76	M	Lambert-Eaton synd.	No significant alteration in the brain
51	M	Acute abdomen	No significant alteration in the brain
PD			
81	F	PD	PD (DLB neocortical type)
84	F	PD	PD (DLB neocortical type)
79	M	PD	PD (DLB neocortical type)
MSA			
68	F	MSA	MSA
82	M	MSA	MSA
71	M	MSA	MSA

PD: Parkinson's disease; DLB: Dementia with Lewy bodies; MSA: Multiple system atrophy

Table S2, related to Figure 8. Clinicopathologic profiles of the patients.

Age at death (yrs)	Sex	Clinical Diagnosis	Pathological Diagnosis
Control			
79	F	Spontaneous CSF leaks	Multiple microinfarcts
90	M	Myopathy	Myopathy
PD			
79	M	PD	PD (DLB neocortical type)
87	F	PD	PD (DLB neocortical type)
80	M	PD	PD (DLB neocortical type)

PD: Parkinson's disease; DLB: Dementia with Lewy bodies; CSF: cerebrospinal fluid

Transparent Methods

Cell lines and culture condition

HeLa and 293T cells were cultured in Dulbecco's modified Eagle's medium (DMEM) supplemented with 10% heat-inactivated fetal bovine serum (FBS), 4 mM L-glutamine, 50 units/ml penicillin, 50 µg/ml streptomycin and MEM Non-essential amino acid (AA) solution (Thermo Fisher Scientific). Neuro-2a is a mouse neuroblastoma cell line, and cells were cultured in DMEM supplemented with 5% FBS, Opti-MEM (Thermo Fisher Scientific), 50 units/ml penicillin, 50 µg/ml streptomycin and MEM Non-essential AA solution.

Preparation of primary rat neuron-enriched cells

Rat primary neuron-enriched cells were prepared as described previously (Iwakura et al., 2017). Cortical tissues were dissected from rat embryos at embryonic days 16–19 and digested with papain (Worthington Biochemical Corporation). Cells were plated on glass coverslips coated with poly-D-lysine (Sigma-Aldrich) in a 6-well plate (Corning), and cells were cultured in DMEM supplemented with 10% FBS. After overnight culturing, the medium was replaced with serum-free DMEM supplemented with the N-2 Supplement (Gibco) and L-glutamine, and cells were further cultured for 4 d. Cells were then treated with 2 µM MG-132 or DMSO for 8 hr, and characterized by immunostaining.

Sprague-Dawley (SD) rats (Japan SLC, Inc., Shizuoka, Japan) were maintained in the animal care facility of the Niigata University Brain Research Institute. All rats were housed in acrylic cages (24 × 39 × 19.5 cm), and they had food and water ad libitum in a temperature-controlled room (23 ± 2 °C) under a 12-hr light:12-hr dark cycle (light from 8:00 am to 8:00 pm). The Animal Use and Care Committee of Niigata University approved this study and all animal experiments described were carried out in accordance with the institutional guidelines and with those of the National Institutes of Health Guide for the Care and Use of Laboratory Animals (NIH Publications No. 80-23). All efforts were made to minimize discomfort to the rats and the number used.

Reagents and antibodies

The following reagents were purchased from the indicated companies: MG-132 (474790; Calbiochem), bortezomib (B-1408; LC Laboratories), bafilomycin A1 (B1793; Sigma-Aldrich), blasticidin (R21001; Thermo Fisher Scientific), puromycin (P8833; Sigma-Aldrich), N-acetylcysteine (A9165; Sigma-Aldrich) and Hoechst 33258 (H-3569; Molecular Probes). The following antibodies were used in this study: anti-USP10 (A300-901A; Bethyl Laboratories, HPA006731; Sigma-Aldrich), anti-ubiquitin (sc-8017; Santa

Cruz Biotechnology), anti-p62 (PM045; MBL, GP62-C; PROGEN), anti-phospho-p62 (pS351) (PM074; MBL), anti-LC3 (PM036B; MBL), anti-HDAC6 (sc-11420; Santa Cruz Biotechnology), anti-G3BP (611127; BD Transduction Laboratories), anti-dynein intermediate chain (D5167; Sigma-Aldrich), anti-LAMP-1 (L1418; Sigma-Aldrich), anti-HA (H9658; Sigma-Aldrich, 3724; Cell Signaling), anti-GFP (sc-9996; Santa Cruz Biotechnology), anti-Nrf2 (sc-13032; Santa Cruz Biotechnology), anti-PSMA3 (ab109532; Abcam), anti-PSMC4 (sc-166003; Santa Cruz Biotechnology), anti-cleaved caspase-3 (9661; Cell Signaling), anti-p53 (sc-126; Santa Cruz Biotechnology), anti-Lamin B (sc-6217; Santa Cruz Biotechnology), anti-Lamin B1 (sc-374015; Santa Cruz Biotechnology), anti- α -synuclein (S5566; Sigma-Aldrich), anti-phosphorylated α -synuclein (015-25191; Wako), anti-synphilin-1 (sc-365741; Santa Cruz Biotechnology) and anti- β -actin (sc-47778; Santa Cruz Biotechnology).

Plasmids

Expression plasmids encoding wild-type USP10 or mutants (USP10^{C424A}, USP10¹⁻¹¹⁶, USP10¹⁻¹⁴⁹, USP10¹⁻¹⁵⁴, USP10¹⁻²¹⁴, USP10¹⁻²⁷⁴, USP10⁹⁶⁻⁷⁹⁸, USP10²¹⁵⁻⁷⁹⁸, USP10²⁷⁵⁻⁷⁹⁸, USP10⁴¹⁰⁻⁷⁹⁸ and USP10⁵⁹⁴⁻⁷⁹⁸) with an N-terminal hemagglutinin (HA) epitope tag were generated by subcloning the respective cDNAs into an expression plasmid pCMV-HA (Clontech). The non-tagged USP10 expression plasmid was generated by subcloning USP10 cDNA into the expression plasmid pcDNA3 (Invitrogen). Retroviral expression plasmid pMXs-puro encoding p62 was used for the expression of exogenous p62. pcDNA3 encoding p53 was used for the expression of human p53. Lentiviral expression plasmids encoding wild-type USP10 or its mutants (USP10^{C424A}, USP10⁹⁶⁻⁷⁹⁸ and USP10¹⁻²¹⁴) with an N-terminal HA epitope tag were generated by inserting the respective cDNAs into CSII-EF-RfA with a blasticidin resistance gene (Higuchi et al., 2007) using Gateway recombination and following the manufacturer's instructions (Gateway System; Invitrogen). The lentiviral short hairpin RNA (shRNA) plasmid pLKO.1-puro targeting human *USP10* with a puromycin resistant gene was purchased from Sigma-Aldrich. pEGFP-LC3 (Kabeya et al., 2000) (Addgene plasmid #21073) was a gift from Tamotsu Yoshimori. YFP-CL1 (Menendez-Benito et al., 2005) (Addgene plasmid #11950) was a gift from Nico Dantuma.

Plasmid transfection

Plasmids (0.5–1.0 μ g) were transfected into HeLa cells (1.5×10^5) on a 6-well plate (Corning) by using the FuGENE 6 reagent according to the manufacturer's instructions (Roche).

Establishment of stable cell lines by viral transduction

Stable knockdowns of endogenous USP10 in HeLa and 293T cells were carried out by using the lentivirus vectors encoding *USP10* shRNA. HIV-1-based lentiviruses encoding *USP10* shRNA were produced by cotransfection of the three plasmids (pLKO.1-puro: 4.28 µg; pCAG-HIVgp: 2.86 µg; pCMV-VSV-G-RSV-Rev: 2.86 µg) into 293T cells (2×10^6) by using the FuGENE HD reagent according to the manufacturer's instructions (Roche), and the viruses were concentrated with Amicon Ultra-15 units (Millipore) to increase the infectious titer of the virus and infected into HeLa or 293T cells in the presence of 8 µg/µl polybrene. These cells were cultured in the selection medium containing 2 µg/ml puromycin.

Lentiviruses encoding wild-type USP10 or its mutants (USP10^{C424A}, USP10⁹⁶⁻⁷⁹⁸ and USP10¹⁻²¹⁴) were established using the same method employed for *USP10* shRNA described above, and used for infection into HeLa cells. These cells were cultured in the selection medium containing 5 µg/ml blasticidin.

RNA interference

Small interfering RNAs (siRNA) specific to human *p62* RNA (Oligo ID: HSS113116, HSS113117) and the negative control siRNA (Cat. No. 12935-100) were purchased from Invitrogen. These siRNA (50-100 pmol) were transfected into cells using Lipofectamine RNAiMAX reagents according to the manufacturer's protocol (Invitrogen).

Coimmunoprecipitation assay

The cells (1.0×10^7) on a 10-cm² dish (Corning) were lysed with ice-cold NP-40 lysis buffer (1% Nonidet P-40, 25 mM Tris-HCl, pH 7.2, 150 mM NaCl, 1 mM EDTA, 1 mM phenylmethylsulfonyl fluoride, 20 µg/ml aprotinin) and cell lysates were treated with the anti-GFP or anti-p62 antibody. Immune complexes were precipitated by protein G-sepharose beads (GE Healthcare). The beads were washed, boiled in sodium dodecyl sulfate (SDS) lysis buffer (62.5 mM Tris-HCl, pH 6.8, 2% SDS, 10% glycerol, 5% 2-mercaptoethanol and 0.005% bromophenol blue) and then released proteins from the beads were subjected to western blot analysis.

Deubiquitination assay

The cells (4.0×10^5) on a 6-cm² dish (Corning) were transfected with the His-ubiquitin and p53 plasmids together with HA-USP10 or its deubiquitinase-dead mutant USP10^{C424A} plasmid. After treatment with 5 µM MG-132 or DMSO for 4 hr, cells were lysed with

buffer A (6 M guanidine-HCl, 0.1 M Na₂HPO₄, 0.1 M NaH₂PO₄, 10 mM imidazole, pH 8.0), and cell lysates were incubated with Ni-NTA-agarose (QIAGEN) at room temperature for 3 hr. This Ni-NTA agarose was sequentially washed with buffer A, buffer A plus B (1:4) and buffer B (25 mM Tris-HCl pH 6.8, 20 mM imidazole), and proteins that bound to the Ni-NTA agarose were eluted by SDS lysis buffer containing 200 mM imidazole. The eluted proteins were then subjected to western blot analysis.

Western blot analysis

The cells were lysed with SDS lysis buffer and cell lysates (20 µg of proteins) were separated by SDS-PAGE, electrophoretically transferred onto a PVDF membrane (Immobilon; Millipore), and treated with the indicated antibodies diluted in Can Get Signal (TOYOBO). Immunoreactive bands were detected with an enhanced chemiluminescence (ECL) detection system (ECL Western Blotting Detection Reagents; GE Healthcare, Pierce™ ECL Plus Western Blotting Substrate; Thermo Fisher Scientific) and were visualized by Amersham Hyperfilm ECL films (Amersham).

Cell fractionation

Three cell lysates (whole-cell extract, soluble fraction and insoluble fraction) were prepared by the following methods. Cultured cells were treated with cold NP-40 lysis buffer, and cell lysates were collected and used as the soluble fraction. The resultant pellet was further treated with the SDS lysis buffer and the lysates were used as the insoluble fraction. Cells were directly treated with the SDS lysis buffer and used as whole-cell extracts. These three lysates were subjected to western blot analysis. Autopsy brain samples from PD patients and the controls were treated with ice-cold Triton X-100 lysis buffer (1% Triton X-100, 50 mM Tris-HCl, pH 7.5, 150 mM NaCl, 1 mM phenylmethylsulfonyl fluoride, 20 µg/ml aprotinin), and the Triton X-100-soluble and Triton X-100-insoluble fractions were collected similarly to the method described above, and two fractions were characterized by western blot analysis.

Immunofluorescence analysis

The cells were cultured on glass coverslips in a 6-well plate, and cells were fixed with 3.7% formaldehyde in PBS and permeabilized by 0.1% Triton X-100 in PBS. Cells were then treated with the primary antibodies, and further incubated with the secondary antibody of either the Alexa488- or Alexa594-conjugated anti-immunoglobulin antibody (anti-mouse, anti-rabbit or anti-guinea pig; Molecular Probes). Cell nuclei were stained with Hoechst 33258. The samples were mounted in Fluoromount/Plus™ (Diagnostic

Biosystems) and the images were analysed with a fluorescence microscope (BZ-8000; KEYENCE).

Microscope analysis

Cells with one large HDAC6/p62-double-positive aggregate (more than 15 μm^2 in size) at the perinuclear region with nuclear deformity were counted as aggresome-positive cells. Cells with multiple small HDAC6-negative/p62-positive aggregates (less than 10 μm^2 in size) were counted as p62-aggregate-positive cells. To measure cells with p62/HDAC6-positive aggresome or p62-positive/HDAC6-negative aggregates, 300 cells in random fields from three coverslips were analysed by staining with anti-HDAC6 and anti-p62 antibodies. Percentages of cells with p62/HDAC6-positive aggresome or p62-positive/HDAC6-negative aggregates were calculated as the ratio of aggresome-positive or p62-aggregates-positive cells relative to total cells. To measure cells with aggresome induced by GFP-CFTR- Δ F508, GFP- α -synuclein/synphilin-1 or HA-AIMP2, at least 300 cells in random fields from three or four coverslips were counted. One large GFP- or HA-positive aggregate (more than 15 μm^2 in size) at the perinuclear region with nuclear deformity was evaluated as an aggresome. Percentages of cells with GFP- or HA-positive aggresome were calculated as the ratio of aggresome-positive cells relative to total cells. To measure the size of p62-aggregate (p62 aggregate (μm^2)), cells were transfected with the p62 expression plasmid and the sizes of p62-aggregates were quantified from 30 randomly selected p62-aggregates using the fluorescent analysis software package (BZ-II analyser; KEYENCE). The number of p62-aggregates per cell was counted from 30 randomly selected cells treated with proteasome inhibitors in the presence or absence of N-acetylcysteine. To measure p62 fluorescence intensity at the aggresome (p62-F at aggresome) or Nrf2 fluorescence intensity at the nucleus (Nrf2-F at nucleus), these fluorescence intensities were measured from 20 randomly selected cells using the BZ-II analyser. Detection of ROS was performed as described previously (Takahashi et al., 2013). Briefly, cells were incubated with 5 μM of 5-(and-6)-chloromethyl-2',7'-dichlorodihydrofluorescein diacetate, acetyl ester (CM-H₂DCFDA; Molecular Probes) for 5 min at 37 °C. The cells were fixed with 3.7% formaldehyde in PBS and the CM-H₂DCFDA-fluorescence intensity per cell was quantified using BZ-II analyser. Twenty cells in random fields were analysed and the data are presented as the mean fluorescence intensity (ROS-F). Two methods were used to measure the level of apoptosis. First, apoptotic cells on coverslips were visualized by an anti-cleaved caspase-3 antibody and then stained cells were counted under a fluorescence microscope. Next, cell nuclei were stained with Hoechst33258 and cells with condensed nuclei were counted under a

fluorescence microscope. Three hundred cells in random fields from three coverslips were analysed (cleaved caspase-3 (%) or condensed nuclei (%)).

Detection of protein aggregates by the ProteoStat dye

The ProteoStat Aggresome Detection Kit (Enzo Life Sciences, NY, USA) was used according to the manufacturer's protocol to detect protein aggregates.

Pathological analysis

The study was performed with the approval of the ethics committees of Niigata University. The autopsied brain tissues of patients with PD ($n = 3$), MSA ($n = 3$) and controls ($n = 3$) were used. Formalin-fixed, paraffin-embedded sections, 4- μm -thick, were immunostained using a rabbit polyclonal antibody against USP10 (HPA006731; Sigma-Aldrich) and a mouse monoclonal antibody against phosphorylated α -synuclein (015-25191; Wako). The deparaffinized sections were incubated with formic acid for 5 min and autoclaved for 10 min at 121 °C in citrate buffer. Immunolabeling was detected using the peroxidase-polymer-based method using the Histofine Simple Stain MAX-PO kit (Nichirei Biosciences) and visualized with a diaminobenzidine/ H_2O_2 solution. Counterstaining was carried out with hematoxylin. For immunofluorescent imaging, primary antibodies were detected by Alexa488- or Alexa568-conjugated anti-immunoglobulin secondary antibodies (appropriately anti-mouse or anti-rabbit; Molecular Probes). These signals were observed under a confocal microscope (FV3000RS; Olympus).

Statistical analysis

Data were analysed with the Student's t -test or one-way ANOVA followed by Tukey's Multiple Comparisons Test using Prism7 software (GraphPad) and are presented as the mean \pm sd.

Supplemental References

Higuchi, M., Tsubata, C., Kondo, R., Yoshida, S., Takahashi, M., Oie, M., Tanaka, Y., Mahieux, R., Matsuoka, M., and Fujii, M. (2007). Cooperation of NF-kappaB2/p100 activation and the PDZ domain binding motif signal in human T-cell leukemia virus type 1 (HTLV-1) Tax1 but not HTLV-2 Tax2 is crucial for interleukin-2-independent growth transformation of a T-cell line. *Journal of virology* 81, 11900-11907.

Iwakura, Y., Wang, R., Inamura, N., Araki, K., Higashiyama, S., Takei, N., and Nawa, H. (2017). Glutamate-dependent ectodomain shedding of neuregulin-1 type II precursors in rat forebrain neurons. *PloS one* 12, e0174780.

Kabeya, Y., Mizushima, N., Ueno, T., Yamamoto, A., Kirisako, T., Noda, T., Kominami, E., Ohsumi, Y., and Yoshimori, T. (2000). LC3, a mammalian homologue of yeast Apg8p, is localized in autophagosome membranes after processing. *The EMBO journal* 19, 5720-5728.

Menendez-Benito, V., Verhoef, L.G., Masucci, M.G., and Dantuma, N.P. (2005). Endoplasmic reticulum stress compromises the ubiquitin-proteasome system. *Human molecular genetics* 14, 2787-2799.

Takahashi, M., Higuchi, M., Matsuki, H., Yoshita, M., Ohsawa, T., Oie, M., and Fujii, M. (2013). Stress granules inhibit apoptosis by reducing reactive oxygen species production. *Mol Cell Biol* 33, 815-829.